https://doi.org/10.5194/essd-2026-691
Preprint. Discussion started: 27 August 2026

Open Access Earth System Science Data Discussions

A Comprehensive Global Ocean Radiocarbon Dataset (1700–2024) for Climate Applications

Nabir Mamnun[1], Branwen Williams[2], Rena Mukherjee[2], Roberta L. Hansman[3], Rolf Sonnerup[4], Nikita Tournebise[5], Tim DeVries[6], and Heather Graven[1]

[1]Department of Physics, Imperial College London, London, UK
[2]Claremont McKenna College, Claremont, CA, USA
[3]Woods Hole Oceanographic Institution, Woods Hole, MA, USA
[4]Joint Institute for the Study of the Atmosphere and Ocean, University of Washington, Seattle, WA, USA
[5]Interdepartmental Graduate Program in Marine Science, University of California, Santa Barbara, CA, USA
[6]Earth Research Institute, University of California, Santa Barbara, CA, USA

Correspondence: Nabir Mamnun (n.mamnun@imperial.ac.uk)

Abstract.

Radiocarbon (^{14}C) in the ocean, reported as fractionation-corrected $\Delta^{14}C$, is a key tracer of circulation, ventilation, and carbon-cycle exchange on decadal to centennial timescales. We present a harmonized global compilation of marine $\Delta^{14}C$ observations spanning 1700–2024, comprising 68,543 measurements from two complementary streams: 58,216 ship-based dissolved inorganic carbon (DIC) bottle samples (1955–2024) and 10,327 biogenic carbonate measurements from corals, bivalves, gastropods, and sclerosponges (1700–2020). The ship-based component builds on the Global Ocean Data Analysis Project (GLODAP) by adding data from additional hydrographic cruises and 68 peer-reviewed studies. The carbonate records provide time-resolved observations at individual sites, including historical periods prior to direct measurements, and they extend coverage to coastal, tropical, and deeper-habitat settings where direct seawater sampling remains sparse. All records were screened for metadata completeness, transcribed into a common reporting framework following Stuiver and Polach (1977), and assigned synthesis quality flags (`DELC14QC`) through primary quality control. Deep-ocean crossover diagnostics are archived separately for user advisory review and do not modify bottle `DELC14QC`. The merged ship-based and biogenic carbonate measurements together span pre-bomb baselines through the modern bomb-^{14}C decline across global ocean basins. Version 1.2026 of the compilation is archived on Zenodo as flat CSV files with a per-contribution source table; release in Linked Paleo Data (LiPD) format is planned. The product captures pre-industrial baselines, the bomb-^{14}C transient and its penetration into the interior ocean, and the post-peak decline through recent decades, and is intended to support ocean ventilation assessments, Earth system model evaluation, and multi-century carbon-cycle synthesis.

1 Introduction

Radiocarbon (^{14}C) is produced in the upper atmosphere through the interaction of cosmic rays with nitrogen atoms. Once formed, ^{14}C mixes with atmospheric CO_2 and enters the ocean through air–sea gas exchange at the surface (Broecker et al., 1960). The distribution of ^{14}C in ocean waters, together with its known radioactive decay rate, provides an important tracer for studying ocean circulation, ventilation timescales, and mixing between different water masses (Adkins et al., 1998; Burke and Robinson, 2012; Lower-Spies et al., 2020; Graven et al., 2012b; Rafter et al., 2022; Skinner and Bard, 2022). In addition to its natural production, large amounts of ^{14}C were produced in the atmosphere during nuclear weapons tests in the 1950s and 1960s that significantly altered the distribution of natural radiocarbon and introduced a strong transient signal (Levin and Hesshaimer, 2000; Hua et al., 2013).

The atmospheric "bomb" ^{14}C signal began to rise around 1955, peaked in the mid-1960s, particularly in the Northern Hemisphere (Hua et al., 2013), and then declined as the bomb testing stopped and bomb-derived ^{14}C mixed into the ocean and terrestrial biosphere (Levin and Hesshaimer, 2000). In recent years, the continued decline of the $^{14}C/C$ ratio in CO_2 has been driven mainly by dilution with ^{14}C-free fossil fuel CO_2, the Suess effect (Levin et al., 2010; Graven et al., 2012c). Invasion of bomb ^{14}C into the ocean has provided strong constraints on air–sea gas exchange and the rate at which surface waters are ventilated into the interior of the ocean (Broecker et al., 1978; Graven et al., 2012b). Observations of natural and bomb-produced ^{14}C can provide key insights into past and present changes in ocean circulation and their influence on global climate variability (Pookkandy et al., 2023; Druffel, 1989; Rafter et al., 2017).

Despite its usefulness, studies applying ^{14}C to study ocean processes are limited by a lack of data. Direct measurements of ^{14}C in seawater are logistically demanding since ^{14}C cannot be measured at sea and, therefore, remain scarce (Key et al., 2004). The distribution of ^{14}C in natural reservoirs for the "pre-bomb" period before atmospheric nuclear weapons tests was not well quantified, as the bomb-produced ^{14}C perturbation occurred soon after the discovery of natural radiocarbon and before extensive measurement surveys of the ocean had begun (Graven et al., 2012a). Indirect measurement approaches that exploit ^{14}C composition recorded in corals, mollusk shells, and sclerosponges have enabled the reconstruction of pre-bomb ^{14}C levels and have extended the radiocarbon record back several centuries. However, these data are also scarce.

The aim of this study is to compile direct measurements and carbonate records of ocean ^{14}C into a comprehensive dataset that can be used in modeling and data analysis, thereby making the data more readily available and maximizing the utility of the scarce data. So far, data compilations for direct and carbonate measurements have been separate and have not included all available data.

The Global Ocean Data Analysis Project (GLODAP; Olsen et al., 2016; Lauvset et al., 2024; Lange et al., 2026) provides the most comprehensive and consistently calibrated set of ship-based ^{14}C observations collected since the Geochemical Ocean Sections (GEOSECS) program (Östlund and Stuiver, 1980), but it does not include some measurements from the literature or from recent cruises. Notably, a large dataset of surface-water ^{14}C data measured by Nydal et al. (1998) is not included in GLODAP. Nor are historical ship-based measurements, including some data of ^{14}C before GEOSECS that were compiled by Graven et al. (2012a) from a range of published studies. For biogenic carbonate records, the time series of marine environmental archive radiocarbon measurements largely focuses on reef-building hermatypic coral records (e.g., Grottoli and Eakin, 2007; DeLong et al., 2025), while there are several compilations from other marine archives including long-lived bivalve mollusks (Scourse et al., 2012) and octocorals (Sherwood et al., 2008).

This study addresses the need for a comprehensive compilation that integrates all available sources of marine and proxy-based ^{14}C observations over the past several centuries. We created a global harmonized compilation of ocean $\Delta^{14}C$ observations

https://doi.org/10.5194/essd-2026-691
Preprint. Discussion started: 27 August 2026

spanning the period 1700–2024. The dataset integrates measurements of ship-based dissolved inorganic carbon (DIC) with radiocarbon records derived from marine taxa with growth that spans decades to several centuries collected from published literature and public repositories. This unified dataset is designed to facilitate improved evaluation of models, ocean processes, and long-term carbon-cycle variability.

2 Data Synthesis

2.1 Δ^{14}C Notation

We use the Δ^{14}C notation for radiocarbon activities, which is the conventional metric used in oceanography. Δ^{14}C refers to the ^{14}C/C ratio, relative to the Modern standard and corrected for mass-dependent isotopic fractionation using δ^{13}C measurements. Δ^{14}C also includes an age correction that accounts for decay between the sampling and analysis dates. A detailed description of radiocarbon reporting conventions is provided in Stuiver and Polach (1977), including the definition of Δ^{14}C, which they refer to as Δ.

2.2 Ship-based Δ^{14}C measurements in dissolved inorganic carbon

Building on the Global Ocean Data Analysis Project (GLODAP), we compile an expanded global dataset of ship-based observations of Δ^{14}C in dissolved inorganic carbon by merging GLODAPv2.2023 (Lauvset et al., 2024) and GLODAPv3 (Lange et al., 2026) and by incorporating additional hydrographic cruises and published literature. Although GLODAPv3 is the more recent GLODAP release, it does not retain the full set of Δ^{14}C bottles present in GLODAPv2.2023. A substantial number of otherwise usable GLODAPv2.2023 measurements are omitted from the GLODAPv3 radiocarbon product because of product-construction and metadata requirements (for example, missing Δ^{14}C in the OCADS source files used by GLODAP, missing accompanying temperature or related fields that cause automated exclusion, or cruise-leg restructuring), rather than because the Δ^{14}C values themselves failed a quality-control assessment. Relying on GLODAPv3 alone would therefore drop many good observations, so we merge the two releases for this synthesis.

We take GLODAPv3 as the baseline and restore GLODAPv2.2023 bottles that have no partner in GLODAPv3. A GLODAPv2.2023 bottle is treated as already present in GLODAPv3 if it matches on cruise and bottle identifiers (`EXPOCODE`, `STATION`, `CAST`, and `BOTTLE`) or, failing that, on cruise identity together with closely matching location and depth (latitude and longitude rounded to 0.01° and depth within a 5 m bin). Bottles without a GLODAPv3 partner—including whole cruises absent from the GLODAPv3 radiocarbon export and unmatched bottles on shared cruise identifiers—are retained from GLODAPv2.2023 and concatenated with the GLODAPv3 baseline to form a merged GLODAP Δ^{14}C table.

Beyond this merged GLODAP foundation, we add Δ^{14}C data from hydrographic cruises archived at the CLIVAR and Carbon Hydrographic Data Office (CCHDO; https://cchdo.ucsd.edu/, last access 30 June 2026) that are not already represented in GLODAP. This includes occupations that remain absent from GLODAPv3 (full cruises, selected stations, and former CCHDO extras), as well as individual bottles omitted from nine cruises that were newly incorporated into GLODAPv3 relative to GLO-

https://doi.org/10.5194/essd-2026-691
Preprint. Discussion started: 27 August 2026

Open Access Earth System Science Data Discussions

DAPv2.2023 but incompletely ingested there; those missing bottles were restored from the corresponding CCHDO archives (Supplementary Table 1). We further include two cruises reported in Castrillejo et al. (2026). In addition, we compile 68 peer-reviewed studies (Supplementary Table 3) not previously included in GLODAP, harmonize their formats and metadata, and integrate them into a consistent dataset. Together, the merged GLODAP product and these additions substantially improve the global coverage and data density of ocean Δ^{14}C observations from 1955 to 2024.

2.3 Δ^{14}C measurements from marine biogenic archives

We compiled measurements of Δ^{14}C from 104 shallow-water hermatypic (zooxanthellate) scleractinian corals, 3 additional azooxanthellate scleractinian corals, and 5 octocoral records whose calcitic skeletons record ambient seawater DIC from previously published articles and data reports (Supplementary Table 4). These corals record the Δ^{14}C of ambient seawater DIC in their calcium carbonate skeletons (Druffel and Linick, 1978; Nozaki et al., 1978). Typically, hermatypic corals have annual density bands that are used to develop a chronology. Seasonal variability in Sr/Ca values sometimes provides a secondary means to determine time in the skeleton. The azooxanthellate scleractinian records extend coverage to deeper waters and higher latitudes poorly represented by shallow hermatypic corals (e.g., Lee et al., 2017; Montero-Serrano et al., 2013). Octocoral (proteinaceous) records are not included in this compilation.

We also compiled growth-band or growth-rate ^{14}C time series records from marine taxa including bivalves, gastropods, and sclerosponges from previously published articles and data reports (Supplementary Tables 5 and 6), which record the radiocarbon content of the ambient seawater and extend the spatial coverage of Δ^{14}C time series to deeper waters, higher latitudes, and regions not represented by coral records alone (e.g., Lower-Spies et al., 2020; Benavides and Druffel, 1986; Dutta et al., 2001).

Ambient DIC is the primary source of carbon to the shells in marine mollusks with typically less than 10% contributed by metabolic CO_2 derived from food sources (Lu et al., 2018; McConnaughey and Gillikin, 2008). Bivalve records are typically cross-dated, providing tight chronological control (Scourse et al., 2006). They are either sessile or have limited mobility, staying within a small area over their lifespan. Compared to bivalves, some gastropods may cover a larger area within their lifespan and have less identifiable annual bands. Thus, gastropod ^{14}C time series were included in this compilation when identified by the original authors as documenting ambient and localized seawater ^{14}C. Sclerosponges derive their carbon from ambient DIC with negligible impact of metabolic CO_2 (Druffel, 1997). Sclerosponges can be found several hundred meters deep in the water column, and while some corals can be found throughout the depths of the worlds oceans, available time series records are typically from specimens within the top 1500 m of the water column. Sclerosponges do not form regularly layered skeletons. Growth chronologies are instead established using ^{210}Pb or U/Th age models or identification of independent tie points in the skeleton and extrapolating growth rates (Rosenheim and Swart, 2007; Fallon and Guilderson, 2005; Grottoli, 2006; Benavides and Druffel, 1986). This introduces uncertainty into the sclerosponge time series chronologies of up to several decades on multi-century long records (Swart et al., 2002). Similarly, while the octocorals have clear annual growth rings in some taxa (e.g., red tree corals, Sherwood et al., 2005), more often the periodicity of growth rings is unknown and techniques similar to

https://doi.org/10.5194/essd-2026-691
Preprint. Discussion started: 27 August 2026

those for sclerosponges are used (Williams and Grottoli, 2010). In the biogenic archives with greater chronological uncertainty, the ^{14}C time series would be most useful in constraining pre-bomb ^{14}C values and not the timing of the bomb curve.

Other sources of ^{14}C from biological archives including measurements from crustose coralline algae, calcified fish tissues, marine mammals, and plankton were not used in this compilation. Several ^{14}C time series from annually banded crustose coralline algae exist but have not yet been peer-reviewed and are not yet publicly available. In fish and marine mammals, the preserved radiocarbon signal often reflects integrated feeding histories rather than ambient seawater conditions, and many species exhibit substantial vertical migration and depth-variable feeding behavior. These ecological factors sometimes introduce large and poorly constrained uncertainties when interpreting fish-based $\Delta^{14}C$ measurements as tracers of water-mass properties. Further, while some plankton including foraminifera provide powerful archives of water mass ^{14}C, studies tend to publish time series records from ocean sediments that extend much further back in time than the scope of this current compilation.

2.4 Quality control

2.4.1 Metadata screening and data standardization

All records entering the compilation were first screened for metadata completeness and harmonized to a common reporting framework. For ship-based DIC $\Delta^{14}C$, GLODAPv2.2023 sampling metadata, harmonized fields, and database quality flags were retained as distributed. Recently archived cruises from CCHDO were converted to World Ocean Circulation Experiment (WOCE) Exchange format (Key et al., 2004), merged with the GLODAPv2.2023 foundation, with GLODAP column headers (fields) adopted as the compilation standard to preserve a consistent structure. Literature-derived DIC measurements (Supplementary Table 3) were extracted from tables, appendices, and supplementary materials, and were formatted to WOCE Exchange where possible.

Missing metadata were encoded with the standard WOCE placeholder (-999). Entries were retained only when each measurement could be traced unambiguously to its source and included sufficient contextual information (location, depth, timing, reported $\Delta^{14}C$ and uncertainty, and reference).

Biogenic records were compiled from peer-reviewed publications, supplementary materials, and public repositories (Supplementary Table 4–6). Measurements were transcribed into a standardized data spreadsheet containing $\Delta^{14}C$, $\Delta^{14}C$ uncertainty, calendar date (year of skeleton formation or sample age assignment), chronological uncertainty where available, and laboratory identifier (`LabID`). A companion metadata sheet assigned each record a unique standardized label and documented species, location, latitude (°N), longitude (°E), depth as stated in the source, depth in meters, record duration, first author and year, DOI, data link, and notes. Individual records were then converted to plain-text profile files with a metadata header followed by the time series of $\Delta^{14}C$, uncertainty, and quality-control flags. Records with incomplete metadata or ambiguous sample provenance were excluded.

Following Stuiver and Polach (1977), all radiocarbon measurements were harmonized to a common notation and reporting framework, with fractionation-corrected $\Delta^{14}C$ and the associated $\delta^{13}C$ (when available) transcribed as reported in each source.

https://doi.org/10.5194/essd-2026-691
Preprint. Discussion started: 27 August 2026

2.4.2 Visual inspection and quality flags

For ship-based DIC Δ^{14}C, we added a synthesis quality column, `DELC14QC`, while retaining the archive flag field `DELC14FLAG` (the GLODAP-equivalent quality flag) unchanged. Measurements already assigned a non-good archive flag at the source were not re-screened; their `DELC14FLAG` values were carried directly into `DELC14QC`. Only bottles that were unflagged in the source archive ($\texttt{DELC14FLAG} \in \{0,2\}$) were candidates for new synthesis flags.

For GLODAPv2.2023 and recent cruises from CCHDO, we first plotted Δ^{14}C versus depth by station and cast to review full vertical profiles. An automated profile check highlighted candidate outliers, which were then inspected visually on these plots; apparent spikes or transcription errors were assigned $\texttt{DELC14QC} = 100$ (synthesis exclusion). Accepted bottles that remained unflagged at the source were assigned $\texttt{DELC14QC} = 2$ (good data).

Literature-derived DIC measurements were screened in the same framework. Studies with vertical structure were reviewed as depth profiles; surface and near-surface-only records were plotted against latitude and longitude and inspected for extreme spikes or obvious transcription errors. As for GLODAP and CCHDO, existing source flags were carried into `DELC14QC` without modification. Literature entries with no source flag were assigned $\texttt{DELC14FLAG} = 0$ at ingest, and accepted measurements were exported with $\texttt{DELC14QC} = 2$.

Biogenic carbonate records were evaluated manually rather than with a uniform automated rule. Each measurement was assessed against regional oceanography, sampling depth, collection period, and large-scale Δ^{14}C structure (pre-bomb baseline, weapons-test peak, and post-bomb decline). Because marine radiocarbon is spatially heterogeneous and not well described by a normal distribution, we did not apply a fixed sigma-based rejection threshold. For banded biogenic carbonate archives, each time series was plotted against a model Δ^{14}C field (Tournebise et al., in prep.) and inspected visually; measurements retained for synthesis use were assigned $\texttt{DELC14QC} = 2$, values requiring caution were assigned $\texttt{DELC14QC} = 10$, and clear outliers or transcription errors were assigned $\texttt{DELC14QC} = 100$. Outliers were defined as measurements judged unusable for global synthesis after visual review—for example physically impossible Δ^{14}C values or clear transcription errors—rather than by a fixed statistical threshold; automated spike detection was used only to highlight candidates for inspection.

Table 1 summarizes the `DELC14QC` values present in the released compilation files.

Table 1. Synthesis quality flags (`DELC14QC`): definitions and counts in the released compilation (version 1.2026).

`DELC14QC`	Recommended use	Ship DIC	Biogenic	Definition
2	Accepted	57,760	10,266	Good measurement retained for synthesis use.
3	Use with caution	247	—	Questionable value; carried from archive `DELC14FLAG` (ship-based DIC only).
6	Exclude	189	—	Bad or unusable value; carried from archive `DELC14FLAG` (ship-based DIC only).
9	Context-dependent	1	—	No data / not measured; carried from source in isolated cases.
10	Use with caution	—	60	Review flag applied after visual inspection of biogenic-carbonate time series.
100	Exclude	19	1	Synthesis exclusion applied after visual inspection (ship-based DIC and biogenic carbonate).
All rows in each CSV		58,216	10,327	

https://doi.org/10.5194/essd-2026-691
Preprint. Discussion started: 27 August 2026

Open Access Earth System Science Data Discussions

2.4.3 Crossover analysis

Crossover analysis compares ship-based profiles (`DELC14QC` = 2) deeper than 1500 m at nearest-neighbor station pairs within 40 km, following GLODAP-style practice (Johnson et al., 2001). This depth cutoff is intended for waters whose Δ^{14}C is nearly stationary between occupations. That assumption does not hold in the North Atlantic, where bomb-produced ^{14}C has continued to invade North Atlantic Deep Water and the Deep Western Boundary Current below 1500 m since the 1990s (Lester et al., 2024). North Atlantic pairs are therefore omitted from the P_{95} baseline and from Figure 5; they remain in the archived crossover table as ventilation-sensitive. Southern Ocean pairs south of 40°S are treated in the same way, while subtropical Pacific and Indian Ocean occupations (depths > 1500 m) are retained. For each pair, profiles are linearly interpolated onto their overlapping depth interval (≥ 200 m span; ≥ 3 matched levels) and depth-level offsets are defined as the more recent cruise minus the earlier occupation. Station-pair offsets are classified into *ok*, *notable*, and *extreme* tiers. The notable threshold is $\max(10‰, P_{95})$ of $|\bar{\Delta}|$ among GLODAP-versus-GLODAP pairs in this Pacific plus subtropical/tropical Indian Ocean domain ($P_{95} = 12.4$ ‰). A fixed advisory extreme cutoff of 20 ‰ is retained; depth levels exceeding twice the combined reported uncertainty are flagged separately. Crossover outcomes are diagnostic only and do not modify bottle `DELC14QC` flags; full results are archived with the dataset (Table 2). Reproducible processing code is provided separately (Code availability).

2.4.4 Internal consistency of biogenic carbonate data

The internal consistency of the compiled biogenic carbonate dataset was further evaluated through comparisons among overlapping records from different archives and measurement programs, including cross-proxy consistency between seawater and biogenic carbonate Δ^{14}C records, repeated sampling at the same or nearby locations, and the temporal coherence of the bomb-^{14}C signal and large-scale spatial gradients. After primary visual inspection (above), each contributing archive was reviewed in regional context using secondary QC time series generated separately for corals, bivalves, gastropods, and sclerosponges: the focal archive record was plotted together with ship-based DIC Δ^{14}C within 250 km and with other biogenic carbonate records within 100 km, in both cases requiring co-location within ±50 m absolute depth and ±5 yr of each archive sample. These contextual overlays supported manual assessment of local coherence but did not automatically modify `DELC14QC`. Detailed internal-consistency assessments, including regional case studies at Galápagos, Daya Bay (South China Sea), and Puerto Rico, are presented in Section 4 (Figure 6), where observational records are also compared against independent datasets and model-based expectations where available.

2.5 Compiled Dataset

2.5.1 File organization

The screened and harmonized marine Δ^{14}C compilation has been archived on Zenodo as CSV files (Mamnun et al., 2026). The deposit is identified by a persistent digital object identifier (DOI) and includes `ship_dic_delta14c_combined.csv` and `delc14_biogenic_carbonate_combined.csv`, which contain the ship-based DIC and biogenic carbonate

https://doi.org/10.5194/essd-2026-691
Preprint. Discussion started: 27 August 2026

measurements, respectively. The tables include the standardized variables, units, uncertainty fields, and harmonized metadata. A comprehensive source table documenting original data sources, sample types, bibliographic references, temporal coverage, and notes for each contributing record has been included in the Zenodo deposit as a spreadsheet and is also provided with this manuscript as Supplementary Material. Table 2 summarizes the files and their contents.

The final compiled dataset will be released in the LiPD (Linked Paleo Data) framework, which provides a standardized, machine-readable structure for paleoclimate and geochemical records. LiPD integrates measurements, uncertainties, metadata, and bibliographic information in a single hierarchical format, supporting transparency and reproducibility and improving interoperability for synthesis, modeling, and data-assimilation workflows. This structure will preserve an explicit link between individual radiocarbon observations, sample metadata, analytical context, and source references in a form that is straightforward to audit and reuse. LiPD will serve as the primary exchange format (rather than, for example, NetCDF) because it is tailored to heterogeneous, multi-archive proxy compilations: it accommodates irregular time series, mixed sample types, and source-specific metadata that are awkward to represent in gridded or strictly regular array models. Following community practice for LiPD-based products, exposure through LiPDverse (or equivalent LinkedEarth-facing discovery services) will occur in line with the journal's data-availability policy and any embargo or versioning requirements tied to the peer-reviewed publication. The LinkedEarth ecosystem emphasizes open, well-documented data products.

Each measurement is intended to be independently auditable through retained source metadata and explicit quality flags on every row. Ship-based entries retain cruise and station identifiers, program tags, original quality flags, and bibliographic links (`SOURCE`, `DOI`) so that individual measurements can be traced to the underlying GLODAP, CCHDO, or literature contribution; biogenic carbonate entries carry equivalent publication identifiers and archive metadata. Compilation-specific screening outcomes are recorded explicitly in `DELC14QC` rather than applied as silent exclusions, so users can reproduce the screened product used in this study or define alternative subsets. Deep-ocean crossover classifications documented in Section 4 are archived separately in Zenodo and are not written back to the main data file. Together with the dataset DOI, these fields pin the exact records underlying the figures and validation analyses reported here.

2.5.2 Versioning and updates

The dataset described in this manuscript is released as version 1.2026. All files distributed through Zenodo and LiPD are versioned and archived with a persistent DOI, ensuring reproducibility of results and traceability of future changes. Any corrections, additions, or modifications to existing records will be published as new and citable versions, while previous versions will remain accessible.

Updated releases may incorporate newly published radiocarbon measurements, extending temporal coverage with additional historical and proxy-based records, and refining metadata and uncertainty estimates as community standards evolve. Each update will be documented through a versioned release with an accompanying change log describing the scope and nature of modifications.

https://doi.org/10.5194/essd-2026-691
Preprint. Discussion started: 27 August 2026

Open Access Earth System Science Data Discussions

Table 2. Available and planned data deliverables and representative variables and metadata.

File / deliverable	Format	Content	Main fields (representative)
README.md	Markdown	Zenodo deposit documentation	File descriptions; column definitions; DELC14QC flag definitions; crossover method summary; citation and contact
compilation_source_index.xlsx	Excel (XLSX)	Per-contribution source index (Zenodo; Supplementary Material)	Worksheets for repeat-survey, literature, coral, mollusk shell, and sclerosponge contributions; source labels; bibliographic references; temporal coverage; notes
ship_dic_delta14c_combined.csv	CSV	Ship-based DIC Δ^{14}C (Zenodo)	Cruise and cast identifiers where available; station metadata; date; coordinates; depth; program flags; Δ^{14}C; uncertainty; δ^{13}C; SOURCE and DOI linking GLODAP, CCHDO, and literature
delc14_biogenic_carbonate_combined.csv	CSV	Biogenic carbonate archives (Zenodo)	Archive type; unique record label; species; location; calendar date; latitude; longitude; depth as stated in the original document and depth in meters; Δ^{14}C and uncertainty; synthesis quality flag; bibliographic source and DOI
LiPD compilation (LiPDverse)	LiPD (JSON + tables)	Planned merged product, hierarchical metadata	Time; latitude; longitude; depth or pressure; archive type; Δ^{14}C and uncertainty; δ^{13}C where reported; units; source tags; provenance and persistent links
delc14_crossover_results.csv	CSV	Deep-ocean crossover diagnostics (Zenodo)	Matched depth-level Δ^{14}C offsets; station-pair tiers; domain flags (QC_DOMAIN, VENTILATION_SENSITIVE); separation; depth-level and literature-review flags; see README.md and Section 2.4.3

CSV, Excel, and documentation files are available from the Zenodo bundle (Mamnun et al., 2026). The LiPD compilation will provide the same semantics in LiPD layout; CSV column labels may differ slightly from future LiPD field names.

3 Dataset overview

This compilation integrates 68,543 measurements of oceanic Δ^{14}C from ship-based dissolved inorganic carbon (DIC) samples and from marine biogenic carbonate archives. The two streams are released as separate CSV files that share a common reporting framework, metadata conventions, and synthesis quality flags (DELC14QC); a single hierarchical LiPD product is planned. The ship-based component includes 58,216 DIC measurements collected between 1955 and 2024, combining GLODAP, CCHDO and other non-GLODAP cruise data, and 68 peer-reviewed studies, and the biogenic carbonate archive component includes 10,327 measurements drawn from 262 contributing records (ages before 1700 excluded from the compiled export). Table 3 summarizes the measurement totals, contributing records, and calendar span by data component, with basin-scale patterns shown in the figures below.

3.1 Ship-based DIC measurements

Ship-based Δ^{14}C observations in DIC are primarily an open-ocean dataset (Figure 1a). Measurements are concentrated along hydrographic sections and repeat occupations, with denser coverage in the North Atlantic and North Pacific and more limited sampling in several regions of the Southern Ocean and parts of the Indian and South Pacific basins. The compilation includes both depth-resolved vertical profiles (circles) and non-profile measurements (triangles), which are dominated by sur-

https://doi.org/10.5194/essd-2026-691
Preprint. Discussion started: 27 August 2026

Open Access Earth System Science Data Discussions

Table 3. Summary of Δ^{14}C data compilation by data component.

Data component	Measurements	Contributing records[a]	Calendar span and coverage
Ship-based measurements of Δ^{14}C in dissolved inorganic carbon (DIC)			
GLODAP	48,205	127	1972–2021; global open ocean, depth-resolved bottle samples and profiles
CCHDO and other cruise data	3,154	20	1999–2024; CCHDO cruises not in GLODAP plus Castrillejo et al. (2026)
Other published studies	6,857	68	1955–2022; global, mostly surface water
Total DIC measurements	**58,216**	**215**	**1955–2024 overall span**
Biogenic carbonate records from marine calcifiers			
Corals	9,790	112	1700–2020; primarily shallow tropical and subtropical reef environments
Bivalves	386	101	1700–2005; shelf and coastal margins across latitudes
Gastropods	52	46	1860–1960; coastal and shelf sites, mainly Indo-Pacific with some Southern Ocean and Atlantic localities
Sclerosponges	99	3	1855–2002; mesophotic to upper bathyal depths where archived
Total calcifier measurements	**10,327**	**262**	**1700–2020 overall span**
All components[b]	**68,543**	**477**	**1700–2024 overall span**

[a]Contributing records denote discrete archive time series or fixed-location compilations; for ship-based DIC, contributing records are summarized where they correspond to clearly delineated cruise/study groupings (68 literature studies in the "Other published studies" row). Biogenic ages before 1700 are excluded from the compiled CSV export. [b]Total observations sum each Δ^{14}C measurement once across components.

face and near-surface samples. Symbol colours distinguish the data sources, highlighting how recent Global Ocean Ship-based Hydrographic Investigations Program (GO-SHIP; Talley et al., 2016) cruises and other recent contributions augment the GLODAPv2.2023 footprint and increase data density along key transects. Although the focus is the open ocean, a small number of coastal surveys and time series are also represented where they are included in GLODAPv2.2023 or available from peer-reviewed studies.

Surface-water Δ^{14}C measurements (depth $\leq$ 50 m) document the uptake of atmospheric bomb-^{14}C by the ocean and its subsequent dilution and redistribution (Figure 1b). The data show ocean Δ^{14}C rising during the 1960s, with the highest values observed after the peak in atmospheric Δ^{14}C in the 1960s. There is substantial scatter that reflects regional differences in air–sea exchange and mixing, with the strongest accumulation of bomb ^{14}C in the subtropical gyres that have weak vertical mixing. In recent years, low- and mid-latitude surface Δ^{14}C exceeds atmospheric $\Delta^{14}CO_2$, reflecting the long ocean memory of the bomb perturbation and the dilution of atmospheric Δ^{14}C by fossil fuel emissions (Lester et al., 2024; Graven, 2015). At

https://doi.org/10.5194/essd-2026-691
Preprint. Discussion started: 27 August 2026

Open Access Earth System Science Data Discussions

high southern and northern latitudes, surface values remain below atmospheric $\Delta^{14}CO_2$ because mixing and upwelling supply older, ^{14}C-depleted waters.

Sampling density is uneven, with comparatively sparse coverage in the 1960s and late 1990s to early 2000s, and comparatively dense coverage in the 1970s and 1990s during the GEOSECS and WOCE intensive hydrographic surveys. Newly compiled data (triangles) increase sampling density and extend coverage relative to GLODAPv2.2023 (circles), improving representation of the 1960s, 1980s, and post-2000 periods.

3.2 Biogenic carbonate archives

Biogenic carbonate archives provide $\Delta^{14}C$ records that extend ocean radiocarbon constraints into the pre-bomb period and complement the ship-based DIC compilation (Figure 2). Sampling locations are globally distributed but concentrated in tropical and subtropical reef settings, with additional coverage from continental margins and mesophotic to upper-bathyal environments where long-lived calcifiers have been recovered (Figure 2a). The time series captures a comparatively stable pre-bomb baseline followed by the rapid rise associated with atmospheric nuclear testing and the subsequent multi-decadal decline (Figure 2b), with measurement density increasing markedly after the 1950s and especially during the decades of intensive post-bomb sampling (1950s–1990s: 1,646, 1,422, 1,539, 1,194, and 734 measurements per decade, respectively, with a further decline to 210 and 83 measurements in the 2000s and 2010s). Regional scatter reflects differences in air–sea exchange, circulation, and upwelling, and some of the lowest post-bomb values are associated with deeper- or mesophotic-habitat archives (e.g., deep corals) that incorporate older, ^{14}C-depleted source waters.

Together, these biogenic carbonate records bridge the transition between sparse pre-bomb observations and the era of widespread ship-based sampling, providing independent constraints on the timing and magnitude of $\Delta^{14}C$ changes in regions and periods where direct seawater measurements are limited.

3.3 Basin-scale coverage

To summarize basin-scale coverage, we partition the full archived product (Table 3) by ocean basin and by the two primary data components of this compilation. Table 4 reports the number of individual measurements in the Atlantic, Pacific, Indian, Southern, and Arctic domains for (i) ship-based DIC $\Delta^{14}C$ observations and (ii) biogenic carbonate archives.

Basin assignment applies polar domains first so that Southern Ocean and Arctic samples are excluded from the Atlantic, Pacific, and Indian columns: measurements south of $40°$S are assigned to *Southern*; measurements at or north of $66.5°$N (Arctic Circle) are assigned to *Arctic*. Remaining samples are partitioned by fixed longitude bands (Atlantic, $80°$W–$20°$E; Indian, $20°$E–$147°$E; Pacific, remaining longitudes). Only rows with valid latitude, longitude, and $\Delta^{14}C$ are included.

Mean ship-based DIC $\Delta^{14}C$ profiles summarize how the bomb-era perturbation and its subsequent redistribution are expressed vertically in each major basin (Figure 3). For each basin, observations are averaged in 18 fixed depth bins from the surface to 6000 m (bin edges and plotting rules as in Figure 3) and grouped by calendar decade (1970s, 1990s, 2000s, and 2010s; one colored curve per decade). Atlantic, Pacific, and Indian domains are assigned from longitude bands after excluding waters south of $40°$S, which are assigned to the Southern Ocean panel. Across basins, upper-ocean $\Delta^{14}C$ in the more recent

https://doi.org/10.5194/essd-2026-691
Preprint. Discussion started: 27 August 2026

Open Access Earth System Science Data Discussions

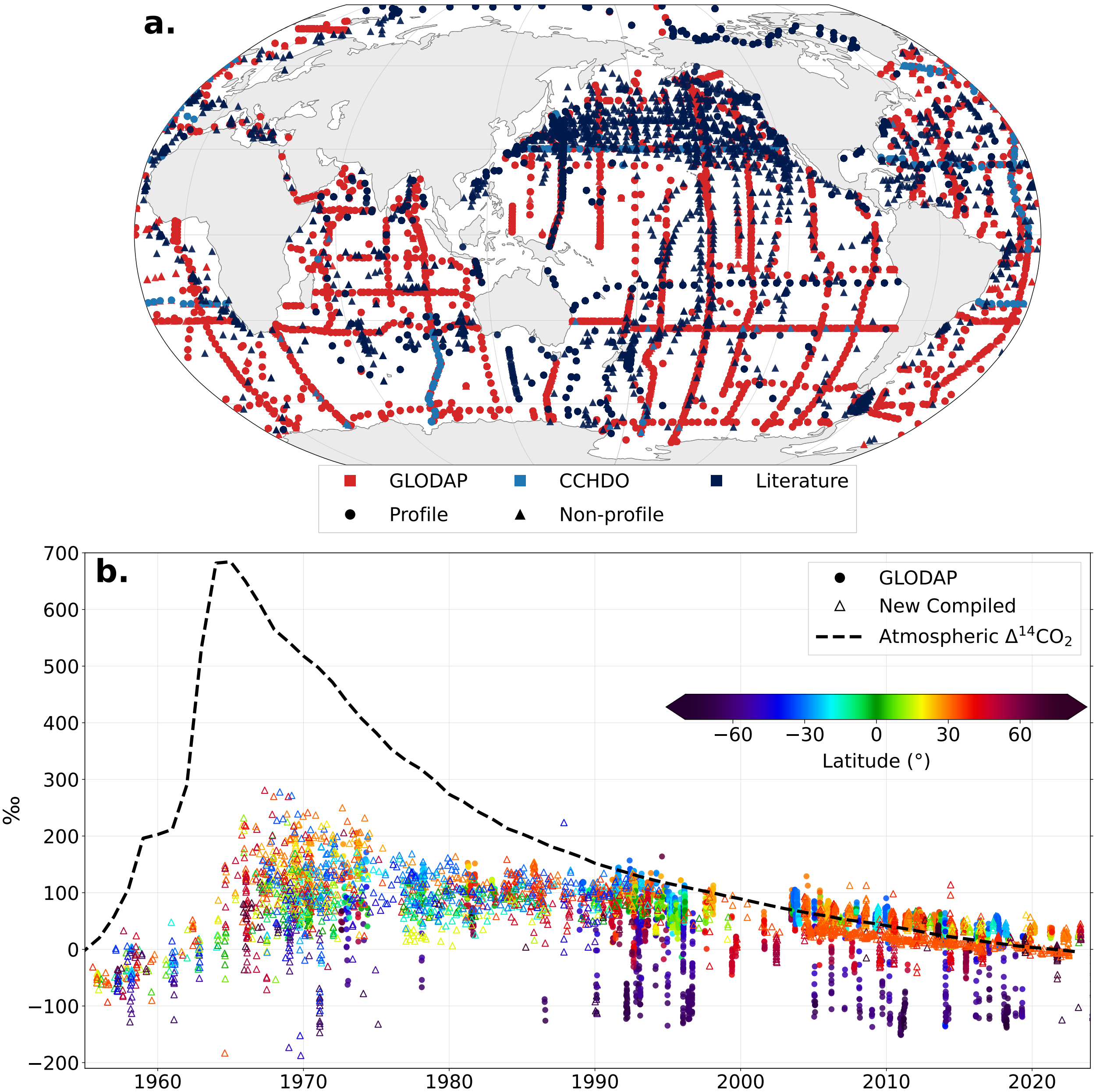

Figure 1. a. Global distribution of ship-based dissolved inorganic carbon (DIC) Δ^{14}C measurements. Circles and triangles distinguish depth-resolved profiles (stations with Δ^{14}C at $\geq$3 distinct depths) and non-profile samples, respectively. Red, blue, and navy symbols mark GLODAP, recent GO-SHIP cruises, and peer-reviewed literature sources compiled here. b. Surface-ocean ($\leq$20 m) Δ^{14}C from 1955 to 2024, with each symbol colored by sample latitude (colour bar). Circles and triangles denote GLODAPv2.2023 and newly compiled measurements, respectively. The black dashed curve shows zonal-mean atmospheric $\Delta^{14}CO_2$ (Graven (2025), updated from Graven et al. (2017)).

https://doi.org/10.5194/essd-2026-691
Preprint. Discussion started: 27 August 2026

Open Access Earth System Science Data Discussions

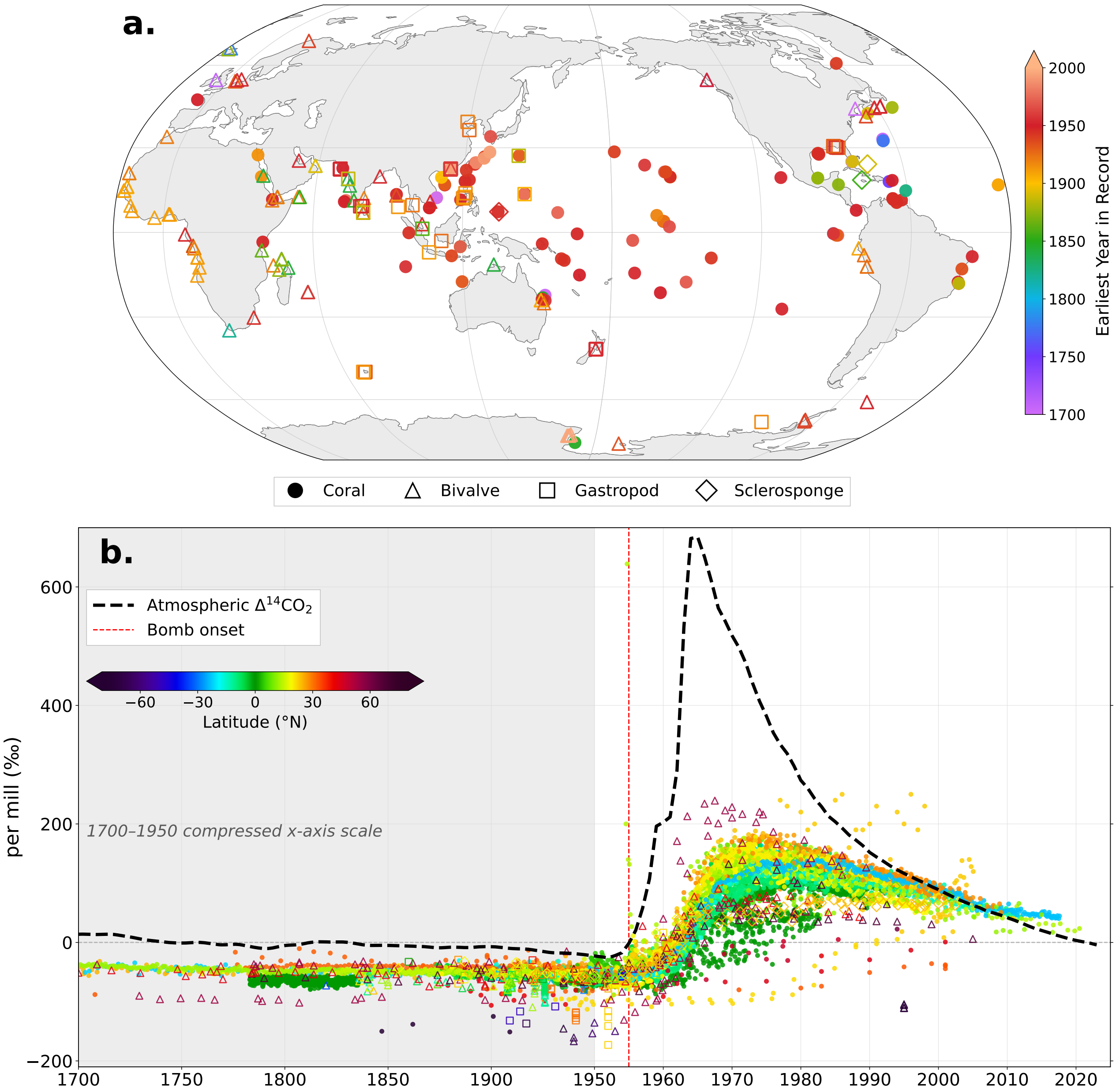

Figure 2. a. Global distribution of biogenic carbonate $\Delta^{14}C$ sampling locations (corals, bivalves, gastropods, and sclerosponges). Each point represents a unique geographic location (latitude and longitude), colored according to the earliest calendar year for which radiocarbon measurements are available at that location. b. Temporal evolution of biogenic carbonate $\Delta^{14}C$ measurements from 1700 to 2020. Each point represents an individual radiocarbon measurement, colored by the latitude of the sampling location. The vertical dashed line at 1955 marks the onset of widespread atmospheric nuclear testing.

https://doi.org/10.5194/essd-2026-691
Preprint. Discussion started: 27 August 2026

Table 4. Basin-scale counts of Δ^{14}C measurements. Atlantic, Pacific, and Indian columns exclude Southern Ocean (south of 40°S) and Arctic (north of 66.5°N) samples.

Data component	Atlantic	Pacific	Indian	Southern	Arctic	Total
Ship-based DIC measurements	11,523	23,498	10,801	11,250	1,144	58,216
Biogenic carbonate measurements	980	5,022	4,261	22	42	10,327
All components	**12,474**	**28,478**	**15,062**	**11,272**	**1,186**	**68,543**

decades exceeds that of the 1970s, consistent with continued bomb-^{14}C uptake and ventilation of surface and mode waters. Deep-water values remain most negative in the Pacific and Indian basins and less depleted in the Atlantic, reflecting basin-scale differences in ventilation and the age of interior water masses. Temporal contrasts are most pronounced in the upper ~1000 m, where the expanded depth scale emphasizes thermocline and mode-water structure; deeper profiles converge toward basin-specific interior values. In the Southern Ocean, decadal curves diverge in the upper ocean but converge below ~1500 m, where Δ^{14}C remains uniformly low.

These decade-mean profiles are exploratory and sampling-sensitive: they are simple depth-bin averages of available bottles, without equal-area weighting, repeat-section pairing, or isopycnal binning, so shifts in cruise tracks between decades can move the basin mean. In the Atlantic, the apparently more depleted deep profile in the 2000s is attributable in large part to a geographic sampling bias toward higher southern latitudes relative to other decades, rather than an Atlantic-wide deep Δ^{14}C decline.

In the Southern Ocean, the near-uniform low Δ^{14}C below ~1500 m is consistent with slow abyssal invasion of bomb ^{14}C, but should not be taken as proof of no downward bomb transport. Stronger quantitative claims about decadal interior change would require repeat sections, isopycnal analyses, or fixed latitude bands.

3.4 Decadal surface distribution

Pre-bomb (1850–1949) and decadal (1950s–2020s) maps of the compiled Δ^{14}C data show how the spatial distribution of Δ^{14}C has changed over time (Figure 4). The data are shown with simulated Δ^{14}C from the CESM2 Large Ensemble (ensemble member 1001; Rodgers et al., 2021) as a backdrop to help visualize the patterns.

In the pre-bomb and 1950s panels, the observations show comparatively weak zonal gradients within each basin, with lower values toward high southern latitudes (e.g., Graven et al., 2012b; Broecker and Olson, 1959). In the 1960s, Δ^{14}C has risen significantly outside of the Southern Ocean with the intrusion of bomb ^{14}C. There is a large scatter in the 1960s as some data are from the early part of the decade when Δ^{14}C had just started to rise and some data are from the late 1960s when some areas had reached peak values of over 150 ‰ (Figures 1 and 2). During the 1970s, the bomb signal becomes more spatially structured: elevated Δ^{14}C appears across subtropical gyres, particularly in the subtropical North Pacific. Strong gradients

https://doi.org/10.5194/essd-2026-691
Preprint. Discussion started: 27 August 2026

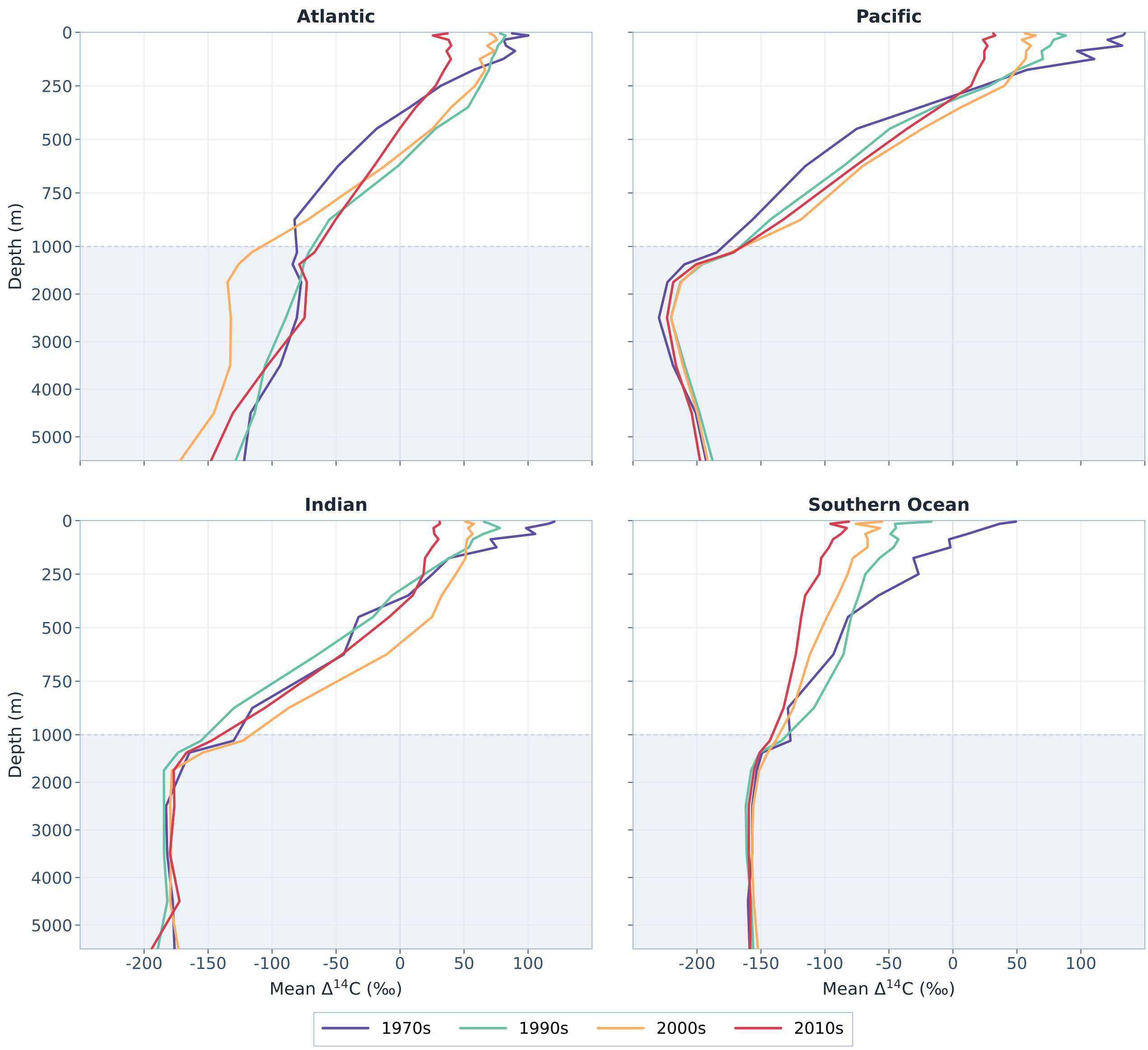

Figure 3. Mean vertical profiles of ship-based DIC $\Delta^{14}C$ by ocean basin and decade. Each panel shows basin-wide mean $\Delta^{14}C$ versus depth. Atlantic, Pacific, and Indian domains are assigned from longitude bands after excluding waters south of 40°S, which are assigned to the Southern Ocean panel. Within each basin, one colored curve is shown for each calendar decade (1970s, 1990s, 2000s, and 2010s); the 1980s are omitted owing to sparse basin coverage. The depth axis uses a piecewise scale that compresses 1000 m–5500 m (shaded). Profiles are depth-bin means for 18 fixed intervals from the surface to 6000 m (bounds at 0, 10, 20, 50, 75, 100, 150, 200, 300, 400, 500, 750, 1000, 1250, 1500, 2000, 3000, 4000, 5000, and 6000 m), plotted at bin midpoints where at least five measurements contribute. Depth increases downward. These decade-mean profiles are exploratory basin averages and are sampling-sensitive; see main text.

between the high-Δ^{14}C gyres and lower-Δ^{14}C ventilation regions in the tropics and higher latitudes create a striped pattern with latitude. From the 1980s through the 2000s these spatial gradients weaken until the 2010s–2020s when the gradients are very weak, similar to pre-bomb gradients, but with higher average Δ^{14}C of about $+50$ ‰ rather than -50 ‰. The lowest Δ^{14}C values persist in the Southern Ocean through all decades.

Our merged ship-based and biogenic carbonate compilation provides a more complete view of surface Δ^{14}C evolution than previously possible. Patterns in pre-bomb and 1950s Δ^{14}C are better defined by our extensive compilation of carbonate records. The 1980s represent another period where the compiled carbonate data are key to defining Δ^{14}C patterns because ship-based DIC data are sparse, particularly in the Pacific. Areas that are enhanced by DIC data from the literature include the Arctic, North Pacific and Southwest Pacific (Figures 1 and 4). The pattern in the North Pacific in the 2000s and 2010s is very well described by compiled observations from GLODAPv2.2023 (Lauvset et al., 2024), repeat GO-SHIP occupations, and northwestern Pacific hydrographic surveys (Kumamoto et al., 2002; Aramaki et al., 2019). Spatial coverage in the Southern Ocean was limited until the 1990s, with the densest coverage in the 2010s.

The changing Δ^{14}C distribution in the observations reflects the uptake and redistribution of bomb ^{14}C in the ocean as well as changes in atmospheric $\Delta^{14}CO_2$ and air–sea gradients. While the CESM2 model shown with the data in Figure 4 generally captures the large-scale patterns, our extended dataset can help to better identify and quantify biases in the model. Frischknecht et al. (2022) found that CESM2 Δ^{14}C underestimated peak surface values relative to coral and bivalve records at roughly twenty sites, but our compiled and merged dataset can better quantify the magnitude and extent of these biases. Lester et al. (2024) and Danabasoglu et al. (2020) identified errors in deep-water formation in CESM2 that cause biases in Δ^{14}C in the deep ocean and at the surface in the Southern Ocean, which could be better quantified with the new dataset. These and other model–data comparisons or model–data integrations will be aided by our comprehensive data compilation.

4 Data Validation

4.1 Radiocarbon crossover analysis

To assess the internal consistency of the compiled ship-based Δ^{14}C dataset, we performed a crossover analysis (Section 2.4.3) for measurements in the deep ocean where Δ^{14}C is not expected to change substantially within a few decades. For the main GLODAP+CCHDO assessment on synthesis-accepted bottles ($\texttt{DELC14QC} = 2$), this analysis yielded 299 station crossovers comprising 4,796 paired deep-water samples across 111 cruise combinations. North Atlantic pairs and Southern Ocean pairs south of 40°S were retained in the archived table but excluded from the GLODAP–GLODAP baseline and from Figure 5, leaving 178 station pairs (3,131 depth levels; 56 cruise combinations) in the Pacific plus subtropical/tropical Indian Ocean.

We emphasize that the global 1500 m depth cutoff follows standard GLODAP-style crossover practice (Johnson et al., 2001) but is not uniformly valid. Oceanic Δ^{14}C has continued to evolve at depths below 1500 m since the 1990s as bomb-produced ^{14}C ventilates the interior (Lester et al., 2024), and this limitation is especially apparent in the Atlantic, where basin-mean vertical profiles show clear decadal changes through the upper thermocline and mode-water depth range (Figure 3). In regions of active ventilation or along North Atlantic Deep Water (NADW) and Deep Western Boundary Current (DWBC) pathways,

https://doi.org/10.5194/essd-2026-691
Preprint. Discussion started: 27 August 2026

Open Access Earth System Science Data Discussions

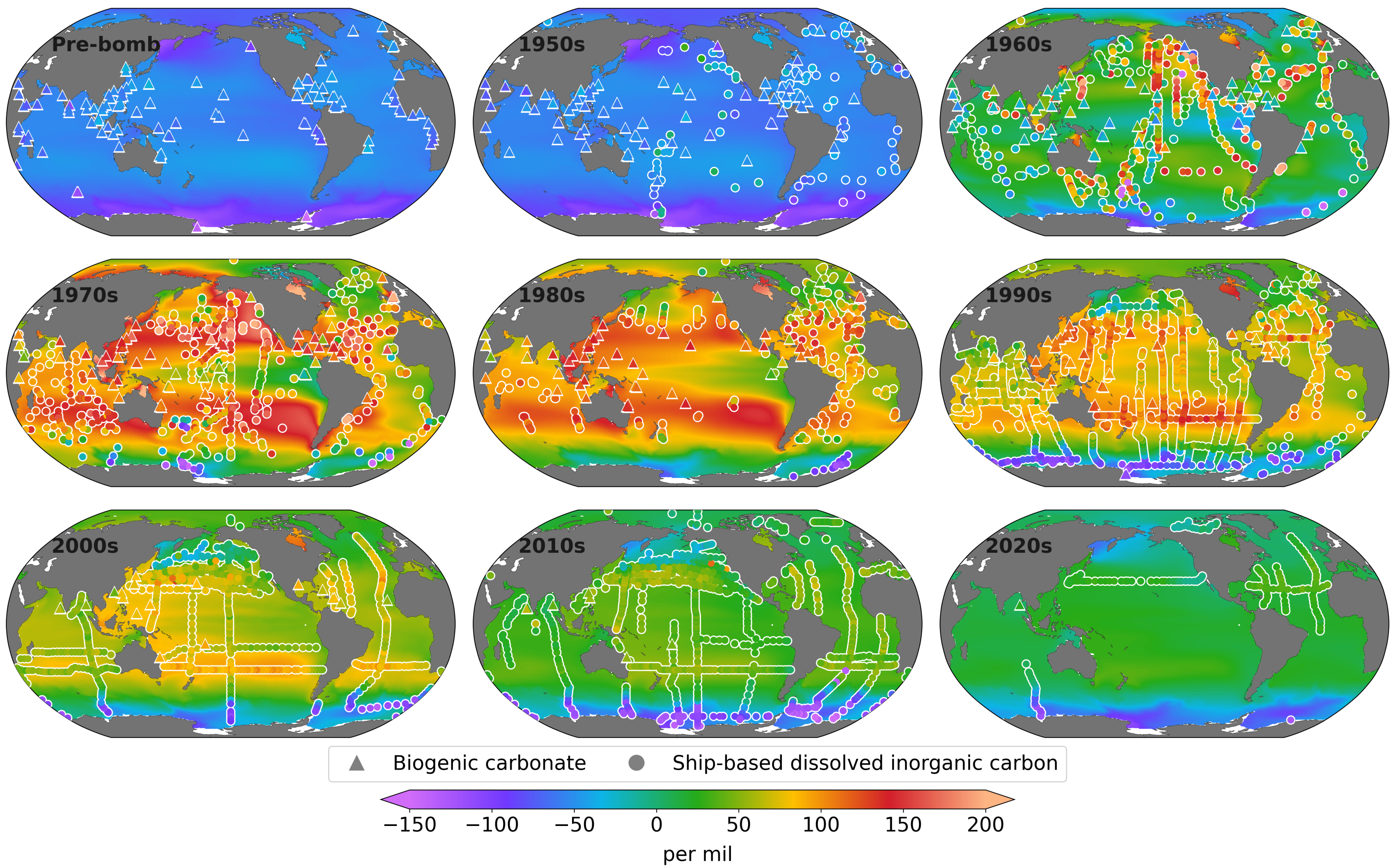

Figure 4. Compiled surface $\Delta^{14}C$ from ship-based dissolved inorganic carbon (circles) and biogenic carbonate archives (triangles), restricted to depth ≤ 50 m where depth is reported and synthesis-accepted (`DELC14QC` = 2). Panels show pre-bomb (1850–1949) and decadal means for the 1950s through the 2020s (left to right, top to bottom). Observations are overlaid on decadal mean surface fields from CESM2 LENS2 member 1001 (Rodgers et al., 2021).

https://doi.org/10.5194/essd-2026-691
Preprint. Discussion started: 27 August 2026

Δ^{14}C can therefore change on decadal timescales even below 1500 m. The offsets reported here should therefore be interpreted as a broad internal-consistency screen rather than as a definitive test of measurement quality in every basin or as evidence of measurement error alone. Regional syntheses may benefit from restricting comparisons to abyssal stable layers (e.g. eastern Atlantic intervals where water-mass Δ^{14}C is demonstrably stationary between occupations; Castrillejo et al. (2024)).

GLODAP-versus-GLODAP crossovers in this Pacific plus subtropical Indian subset ($n = 154$ station pairs) provide the empirical baseline for expected deep-water scatter: the median offset is -0.1 ‰, the median absolute deviation is 3.6 ‰, and the 95th percentile of $|\bar{\Delta}|$ is 12.4 ‰, where $\bar{\Delta}$ is the mean offset at a crossover station pair. The corresponding global GLODAP–GLODAP distribution ($n = 255$) has $P_{95} = 16.9$ ‰, inflated by North Atlantic pairs. We therefore did not apply a single fixed per mil cutoff to reject data automatically. Instead, crossover pairs were assigned to three tiers (Section 2.4.3): *ok* ($|\bar{\Delta}| < 12.4$ ‰), *notable* ($12.4 \leq |\bar{\Delta}| < 20$ ‰), and *extreme* ($|\bar{\Delta}| \geq 20$ ‰). The notable threshold is defined as $\max(10‰,\ P_{95,\mathrm{GLODAP/GLODAP}}) = 12.4‰$ on the QC-domain baseline. The extreme threshold is a fixed advisory cutoff of 20 ‰, above the QC-domain GLODAP–GLODAP tail (no such pair reaches 20 ‰). At the depth level, individual samples were additionally flagged when $|\Delta| > 2\sigma_{\mathrm{combined}}$, where $\sigma_{\mathrm{combined}}$ is the quadrature sum of reported Δ^{14}C uncertainties; these `DEPTH_FLAG` values are diagnostic only and were not propagated to bottle `DELC14QC`. Applying these thresholds to the Pacific plus subtropical Indian GLODAP+CCHDO crossovers yielded 169 *ok*, 9 *notable*, and 0 *extreme* station pairs. The archived global table still contains North Atlantic and Southern Ocean pairs, including the previous extreme offsets; no measurements were removed from the synthesis solely on the basis of crossover magnitude.

Figure 5 summarizes the distribution of crossover offsets for the 20 QC-domain cruise pairs with the largest number of matched deep samples. For most Pacific and subtropical Indian repeat occupations, median offsets cluster near zero, indicating broad consistency between cruises separated by one to three decades (e.g. P17N, P02, P01, and I03). Spread within individual pairs reflects remaining measurement or inter-cruise calibration differences as well as residual water-mass variability; P06 and I08S show wider interquartile ranges than tightly repeated sections such as P17N. QC-domain notables include P17N versus P17C, P06 (2009–10 versus 1992), and P10 (2005 versus 1993); none reach the 20 ‰ extreme tier. North Atlantic repeats such as A20 (2021 versus 1997) and A16N (2013 versus 1993) remain in the archived table as ventilation-sensitive pairs, consistent with bomb ^{14}C on NADW (Lester et al., 2024), and are not shown in Figure 5. Overall, the QC-domain crossover results support the use of the merged GLODAP+CCHDO dataset for deep-water synthesis in the Pacific and subtropical Indian Ocean while highlighting line–year combinations that warrant additional scrutiny.

The same crossover framework was extended to the full ship-based compilation (all sources with $\texttt{DELC14QC} = 2$), using identical profile-comparison rules at the same 40 km search radius. Literature crossovers were not restricted to the Pacific QC domain. Twenty literature or non-GLODAP studies yielded at least one crossover against GLODAP or CCHDO ($n = 54$ station pairs, 541 depth-level comparisons). Castrillejo et al. (2026) contributed the largest number of literature crossovers ($n = 14$ pairs) and showed a mean offset of $+11.9$ ‰ (median $+9.1$ ‰) relative to nearby GLODAP profiles. Most Castrillejo crossovers fell below the extreme threshold, consistent with a systematic positive bias rather than random scatter. Two Castrillejo station pairs on A05 (2020 vs. AR01 1998) exhibited extreme offsets ($+26$ and $+30$ ‰) that were also inconsistent with the other Castrillejo crossovers; these were flagged *questionable* for manual review but retained in the bottle compilation. One

https://doi.org/10.5194/essd-2026-691
Preprint. Discussion started: 27 August 2026

additional literature pair (Dutta, Sagar Sampada 152 vs. I09N 1995) was flagged *questionable* for the same reason. Other literature sources with limited crossover coverage showed near-zero to moderately positive mean offsets at the available stations.

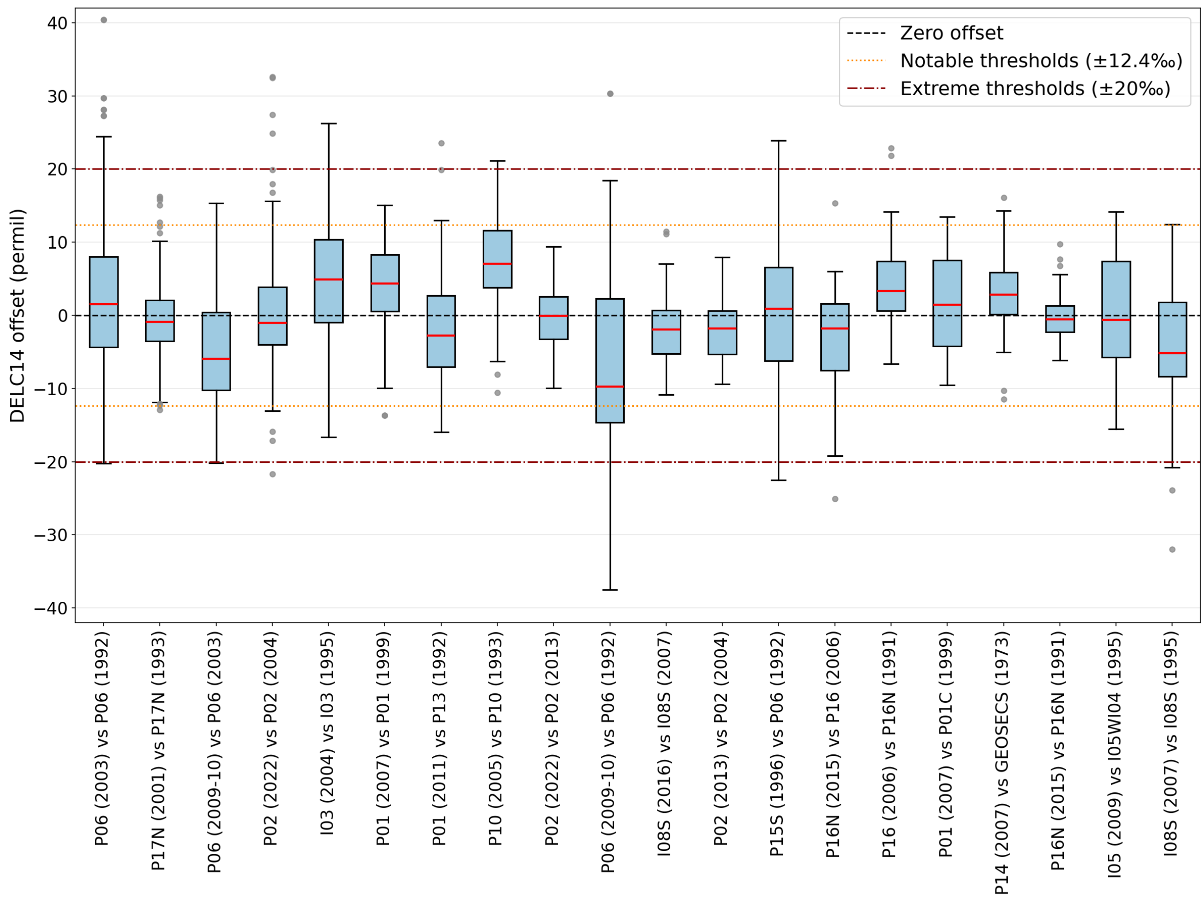

Figure 5. Distribution of deep-ocean Δ^{14}C crossover offsets by cruise pair in the Pacific plus subtropical/tropical Indian QC domain. Boxplots show all matched depth-level offsets for the 20 cruise pairs with the largest number of crossover samples in that domain ($n = 2{,}407$ samples from 131 station crossovers across 20 cruise pairs). Horizontal red lines mark medians; boxes span the interquartile range; whiskers extend to $\pm 1.5 \times$ IQR; grey points are outliers. The dashed horizontal line indicates zero offset. Comparisons use synthesis-accepted bottles ($\texttt{DELC14QC} = 2$), are restricted to depths > 1500 m, require ≥ 200 m overlapping depth span, and ≥ 3 matched levels per station pair within 40 km (Section 2.4.3). North Atlantic pairs and Southern Ocean pairs south of 40° S are excluded from this figure and from the P_{95} baseline (Section 4.1). Depth-level offsets are obtained by linear interpolation onto the union of bottle depths within each station pair's overlapping interval (Section 2.4.3). Dotted horizontal lines at ±12.4 ‰ and ±20 ‰ indicate the notable and extreme tier thresholds derived from the QC-domain GLODAP-versus-GLODAP baseline (Section 2.4.3).

https://doi.org/10.5194/essd-2026-691
Preprint. Discussion started: 27 August 2026

Open Access Earth System Science Data Discussions

4.2 Internal consistency of biogenic carbonate archives

The internal consistency of the compiled carbonate dataset was evaluated through comparisons among overlapping records from different archives and measurement programs, including cross-proxy consistency between seawater and biogenic carbonate archive Δ^{14}C records, as well as repeated sampling at the same or nearby locations. The temporal coherence of the bomb-^{14}C signal and large-scale spatial gradients were used as additional consistency indicators.

In the global biogenic carbonate time series (Figure 2b), the post-bomb segment of the Galápagos record of Druffel et al. (2015) (Urvina Bay, Isabela Island) appears lower than many coeval tropical coral measurements. That pattern is visually pronounced because Figure 2b aggregates all archive types and latitudes on one axis, so site-specific offsets—here, radiocarbon-depleted water associated with persistent equatorial upwelling on the western Galápagos margin—can resemble a compilation artefact rather than a regional signal. To test whether the Galápagos entries are internally consistent, we extracted all biogenic carbonate Δ^{14}C records within 250 km of a central Galápagos anchor (1°S, 90°W), computed calendar-year means for each contributing archive series, and overlaid shallow ship-based DIC Δ^{14}C from the same search window (depth $\leq$50 m) (Figure 6a).

Five independent coral time series are available in this region: Druffel (1981) (Duncan Island), Brown et al. (1993) (San Cristóbal), Druffel and Griffin (1993), Guilderson and Schrag (1998), and Druffel et al. (2015) (Urvina Bay). Despite differences in exact sampling location and pre-bomb coverage, the annual-mean archive curves rise in phase through the weapons-test era and reach comparable peak values in the 1970s–1980s (Figure 6a). The Urvina Bay record of Druffel et al. (2015) remains offset to lower Δ^{14}C during the 1940s–1950s, consistent with its upwelling-influenced setting, but it joins the regional bomb-rise trajectory rather than diverging from the other Galápagos corals. Four surface DIC samples from Nydal et al. (1998), collected between 1989 and 1993 (Δ^{14}C = 50–68 ‰ with reported uncertainties of 4–5 ‰), fall within the envelope of the contemporaneous coral data. We therefore interpret the apparently low Galápagos values in Figure 2b as a site-specific upwelling signature. Together, the regional overlay supports retention of all five Galápagos coral records in the harmonized product.

A second case study addresses overlapping coral records at Daya Bay in the South China Sea (Figure 6b). The Shen et al. (2004) and Wang et al. (2017) profiles sample the same regional shelf system within 250 km of 22.55°N, 114.55°E but span different calendar intervals and show distinct absolute offsets. Secondary QC therefore compared the two profiles against each other: measurements with clear visual inconsistencies were assigned DELC14QC = 10, additional coastal highs inconsistent with the overlapping record were assigned DELC14QC = 10 through inter-profile regional comparison.

At Puerto Rico (Figure 6c), the Vieques coral series of Kilbourne et al. (2007) was originally validated against other coral archives, although not all of those comparison records were from immediately adjacent sites. We therefore overlaid shallow ship-based DIC Δ^{14}C within the same 250 km search window (depth $\leq$50 m; $n = 15$) as an independent cross-proxy check. The ship-based and biogenic records rise and decline in parallel through the bomb era, demonstrating consistency between the two data types in this region.

https://doi.org/10.5194/essd-2026-691
Preprint. Discussion started: 27 August 2026

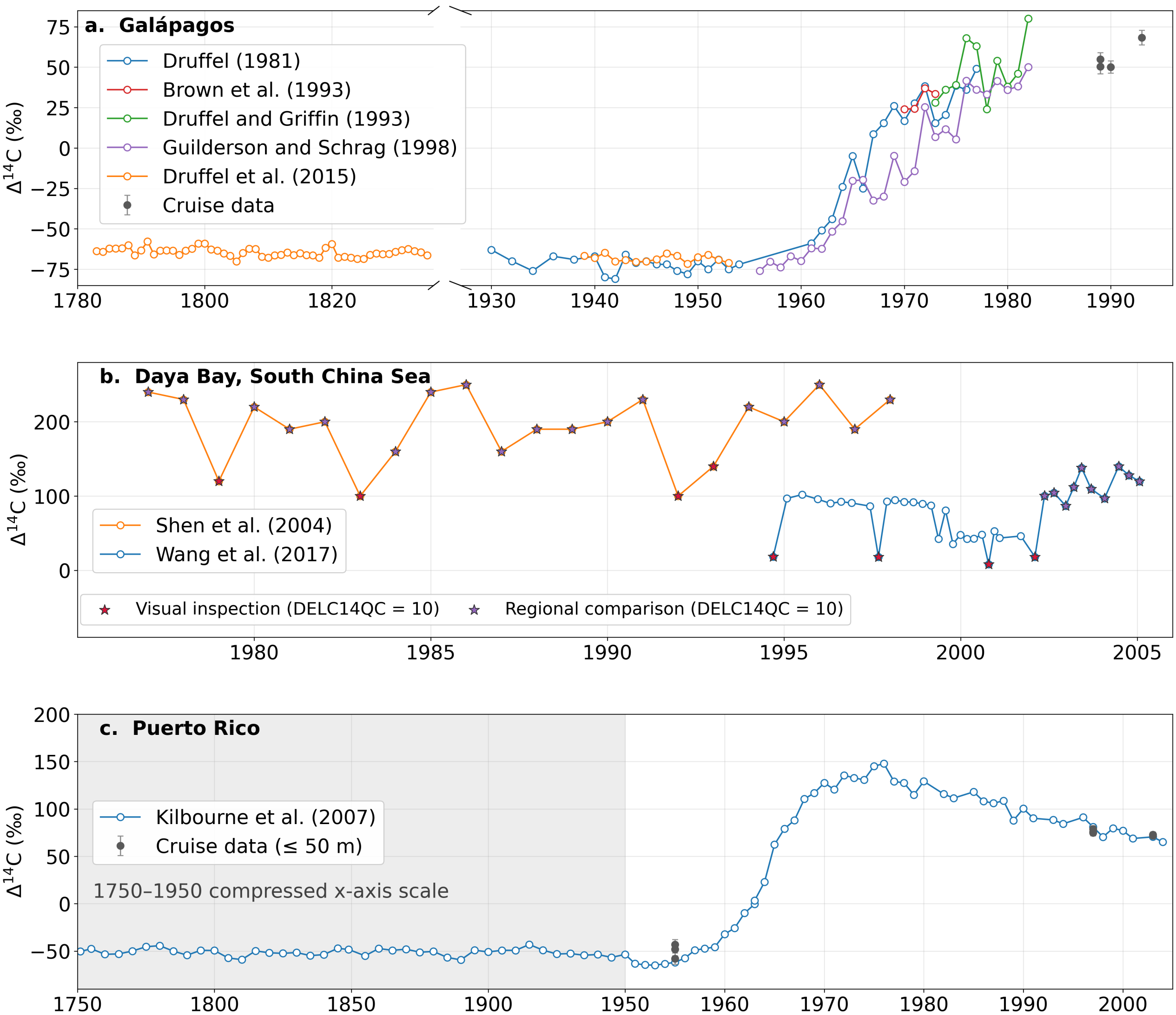

Figure 6. Regional internal-consistency checks for biogenic carbonate Δ^{14}C records. **a. Galápagos:** calendar-year means of coral archives within 250 km of 1°S, 90°W: Druffel (1981) (blue), Brown et al. (1993) (red), Druffel and Griffin (1993) (green), Guilderson and Schrag (1998) (purple), and Druffel et al. (2015) (orange; Urvina Bay). The Druffel et al. (2015) pre-industrial segment (1780–1840) is shown in the left panel; the x-axis is broken before the bomb-era panel (1930–1998). Grey symbols with vertical error bars denote shallow (≤50 m) ship-based DIC Δ^{14}C from Nydal et al. (1998) ($n = 4$, 1989–1993). **b. Daya Bay, South China Sea:** coral Δ^{14}C from Shen et al. (2004) (orange) and Wang et al. (2017) (blue) within 250 km of 22.55°N, 114.55°E. Crimson stars mark values flagged `DELC14QC` = 10 by visual inspection; purple stars mark values flagged `DELC14QC` = 10 by inter-profile regional comparison. **c. Puerto Rico:** coral Δ^{14}C from Kilbourne et al. (2007) (blue) within 250 km of 18°N, 67°W, with shallow (≤50 m) ship-based DIC overlaid (grey symbols with vertical error bars; $n = 15$). The 1750–1950 segment uses a compressed x-axis scale (shaded). Panel (a) complements the global biogenic carbonate summary (Figure 2b), where the Urvina Bay record can appear anomalously low when all latitudes and archive sites are plotted together.

https://doi.org/10.5194/essd-2026-691
Preprint. Discussion started: 27 August 2026

Open Access Earth System Science Data Discussions

4.3 Geographic contrasts in decadal surface maps

Several features in the decadal surface maps (Figure 4) stand out as sharp local contrasts against the regional model backdrop or against co-located measurements from a different platform. The examples below were examined in the context of the synthesis-accepted record (DELC14QC = 2) to aid interpretation of spatial heterogeneity; they do not reflect additional quality-control actions on the harmonized product.

The 2010s North Pacific panel shows elevated ship-based Δ^{14}C along repeat hydrographic lines and in the northwestern Pacific survey of Aramaki et al. (2019) (up to $\sim$114 ‰), while other bottles at similar latitudes are lower—including strongly depleted surface values from repeat occupations off northern Japan (Kaizer et al., 2020) (to ~-41 ‰)—illustrating the sharp meridional gradients resolved by dense repeat hydrography along the western boundary. In the South Atlantic, GLODAP occupations in the 2010s include values near -136 ‰ off the Brazil margin, consistent with strong upwelling of ^{14}C-depleted source waters and contrasting with more positive values in the tropical Atlantic during the same decade. In the 2010s Arctic panel, shallow ship-based Δ^{14}C spans a wide range (from ~-35 ‰ in the Chukchi/Beaufort sector to $\sim$50 ‰ in the Eurasian Arctic; Druffel et al. (2017)), reflecting strong regional ventilation contrasts in a domain where observations remain sparse.

Near Bermuda, shallow reef carbonate records from Goodkin et al. (2012) can appear lower than co-located ship-based DIC from Druffel et al. (1992) on the decadal maps, reflecting regional mode-water and ventilation structure rather than an inconsistency introduced by the merge. In the Galápagos, low biogenic carbonate Δ^{14}C values on the decadal maps are consistent with the regional overlay in Figure 6a and with the strong equatorial upwelling signal documented for Urvina Bay corals (Druffel, 1981; Druffel et al., 2014); Druffel et al. (2014) showed that seasonal Δ^{14}C variability at this site tracks upwelling and tropical climate indices.

A number of historical literature compilations contribute values outside the -150 ‰ to 200 ‰ range used for map colour scaling, including high bomb-era measurements from Fairhall and Young (1985) and Nydal et al. (1998) in the Pacific, from Linick (1978), and very negative Southern Ocean values from Vogel and Marais (1971). North Sea bivalve records from Weidman (1995) also reach higher Δ^{14}C than surrounding ship-based fields in the 1960s–1970s. These end-member values were retained in the synthesis after primary QC and are visible on the decadal maps only at the colour-scale limits; full magnitudes are reported in the archived CSV files.

5 Code and data availability

The global ocean Δ^{14}C data compilation (version 1.2026) is available from Zenodo at https://doi.org/10.5281/zenodo.18674659 (Mamnun et al., 2026). The repository comprises CSV files (`ship_dic_delta14c_combined.csv` for ship-based DIC measurements, `delc14_biogenic_carbonate_combined.csv` for biogenic carbonate archives, and `delc14_crossover_results.csv` for deep-ocean crossover diagnostics); `compilation_source_index.xlsx`, a per-contribution source table documenting bibliographic references, sample types, temporal coverage, and compilation notes, and `README.md`. Field definitions, quality flags, and provenance links for individual measurements are described in `README.md`.

https://doi.org/10.5194/essd-2026-691
Preprint. Discussion started: 27 August 2026

The same compilation will subsequently be released in Linked Paleo Data (LiPD) format through the LinkedEarth ecosystem, with discovery and landing pages on the LiPDverse data portal. That LiPD product will encode the merged ship-based and archive streams in a hierarchical, machine-readable layout suited to multi-archive synthesis and model–data workflows, and will be assigned its own citable DOI once published. Until the LiPD release is available, users should cite the Zenodo deposit above, or this paper.

The Python scripts and Jupyter notebooks used to compile the Zenodo CSV products, assign synthesis quality flags (`DELC14QC`), run deep-ocean crossover analysis, and generate manuscript figures are available in Zenodo at https://zenodo.org/records/22100029 Mamnun (2026). A version-pinned Zenodo software deposit with its own DOI, separate from the data product (Mamnun et al., 2026), will be added in a future release.

6 Conclusions

We presented a harmonized global compilation of marine Δ^{14}C observations covering 1700–2024, integrating 68,543 measurements from two complementary streams: 58,216 ship-based DIC observations (1955–2024) and 10,327 biogenic carbonate measurements from corals, bivalves, gastropods, and sclerosponges (1700–2020). All records were transcribed into a common framework with aligned metadata (location, depth, time, archive type, uncertainty, and provenance), enabling consistent synthesis, mapping, and model–data evaluation across heterogeneous sources.

This merged archive broadens observational constraints across the full marine Δ^{14}C trajectory, from pre-industrial baselines through the bomb ^{14}C uptake period and into the modern decline. The combined surface record also improves the uneven decadal measurement density in hydrographic survey data in GLODAP and provides a more complete picture of the pre-bomb Δ^{14}C distribution, including the decadal surface patterns.

The merged compilation provides a substantially expanded observational basis for model–data evaluation of marine radiocarbon across Earth system models by integrating ship-based DIC and biogenic carbonate records in a single harmonized framework with shared metadata and primary synthesis quality flags (`DELC14QC`), supporting consistent comparison with simulated surface and near-surface Δ^{14}C from pre-bomb baselines through the bomb-era transient and into the modern decline. Deep-ocean crossover diagnostics are archived for user advisory review only and do not modify `DELC14QC`.

As an illustration, overlaying synthesis-accepted observations on CESM2 LENS2 member 1001 (Figure 4) shows how the compilation extends prior assessments based on GLODAP and a limited set of archive records (Frischknecht et al., 2022; Lester et al., 2024), while remaining broadly consistent with previously reported model offsets in upwelling domains and subtropical gyres.

By creating the most comprehensive Δ^{14}C measurement compilation, we provide a tool that can be used for multiple purposes, including evaluating ocean circulation, tracer transport, and carbon-cycle exchange. We expect the dataset to expand as new cruises and marine archive records become available and we invite community input to add to and improve the dataset.

https://doi.org/10.5194/essd-2026-691
Preprint. Discussion started: 27 August 2026

Author contributions. NM: conceptualization, data curation, formal analysis, validation, visualization, writing – original draft preparation, writing – review and editing. BW: conceptualization, data curation, validation, writing – original draft preparation, writing – review and editing, supervision, funding acquisition. RM: data curation, validation, writing – original draft preparation. RH: validation, writing – review and editing. RS: validation, writing – review and editing. NT: visualization, validation, writing – review and editing. TD: conceptualization, writing – review and editing, funding acquisition. HG: conceptualization, data curation, validation, writing – original draft preparation, writing – review and editing, supervision, funding acquisition.

Competing interests. The authors declare that they have no conflict of interest.

Acknowledgements. We thank the many scientists, technicians, and crews who collected, analysed, and archived the radiocarbon measurements compiled in this study. We gratefully acknowledge the Global Ocean Data Analysis Project (GLODAP; https://glodap.info/) and its international community of contributors, whose GLODAPv2.2023 product forms the foundation of this compilation. Additional hydrographic Δ^{14}C data were obtained from the CLIVAR and Carbon Hydrographic Data Office (CCHDO; https://cchdo.ucsd.edu/). We thank the chief scientists, officers, crew, and scientific parties of the cruises listed in Supplementary Table 1, as well as the US Global Ocean Ship-based Hydrographic Investigations Program (US GO-SHIP), GEOTRACES, and international partner programmes that supported them. We also thank the authors of the studies listed in Supplementary Tables 3-6 for making their ^{14}C records publicly available, and M. Castrillejo and colleagues for sharing data prior to publication. We also thank Dr. Angelica Pasqualini for sharing numeric data from Schlosser et al. (1994) and Schlosser et al. (1997), Dr. Patrick Rafter for sharing data from Rafter et al. (2017), and Dr. Nathalie Goodkin for sharing coral data from Goodkin et al. (2012). Some coral, mollusk shell, and sclerosponge Δ^{14}C records were obtained from the NOAA National Centers for Environmental Information (NCEI) World Data Service for Paleoclimatology (https://www.ncei.noaa.gov/products/paleoclimatology) and the PANGAEA Data Publisher for Earth and Environmental Science (https://www.pangaea.de/). We acknowledge the data contributors and the data stewards of both archives for curating and openly distributing these records. We are grateful to the CESM2 Large Ensemble Community Project and supercomputing resources provided by the IBS Center for Climate Physics in South Korea. We acknowledge the use of large language models (ChatGPT and Gemini) for coding suggestions, transcription of large tables, and wording suggestions in some cases; the authors reviewed and verified all outputs.

Financial support. This work is a contribution of the Integration of Models and Observations across Scales (InMOS) project, supported by Schmidt Sciences, LLC and NSF MGG and CO award 2322042 to BW.

References

Adkins, J. F., Cheng, H., Boyle, E. A., Druffel, E. R. M., and Edwards, R. L.: Deep-Sea Coral Evidence for Rapid Change in Ventilation of the Deep North Atlantic 15,400 Years Ago, Science, 280, 725–728, https://doi.org/10.1126/science.280.5364.725, 1998.

Aramaki, T., Mizushima, T., Kuji, T., Povinec, P. P., and Togawa, O.: Summer Surface Water Radiocarbon in the North Pacific Ocean, 2004–2016, Radiocarbon, 61, 1367–1375, https://doi.org/10.1017/RDC.2019.32, 2019.

Benavides, L. M. and Druffel, E. R. M.: Sclerosponge growth rate as determined by 210Pb and 14C chronologies, Coral Reefs, 4, 221–224, https://doi.org/10.1007/BF00298080, 1986.

Broecker, W. S. and Olson, E. A.: Lamont Radiocarbon Measurements VI, Radiocarbon, 1, 111–132, https://doi.org/10.1017/S0033822200020427, 1959.

Broecker, W. S., Gerard, R., Ewing, M., and Heezen, B. C.: Natural radiocarbon in the Atlantic Ocean, Journal of Geophysical Research, 65, 2903–2931, https://doi.org/10.1029/JZ065i009p02903, 1960.

Broecker, W. S., Peng, T. H., and Stuiver, M.: An estimate of the upwelling rate in the equatorial Atlantic based on the distribution of bomb radiocarbon, Journal of Geophysical Research: Oceans, 83, 6179–6186, https://doi.org/10.1029/JC083iC12p06179, 1978.

Brown, T. A., Farwell, G. W., Grootes, P. M., Schmidt, F. H., and Stuiver, M.: Intra-Annual Variability of the Radiocarbon Content of Corals from the Galapagos Islands, Radiocarbon, 35, 245–251, https://doi.org/10.1017/S0033822200064912, 1993.

Burke, A. and Robinson, L. F.: The Southern Ocean's Role in Carbon Exchange During the Last Deglaciation, Science, 335, 557–561, https://doi.org/10.1126/science.1208163, 2012.

Castrillejo, M., Hansman, R. L., Graven, H. D., Lester, J. G., Bollhalder, S., Kündig, K., and Wacker, L.: Comparability of radiocarbon measurements in dissolved inorganic carbon of seawater produced at ETH-Zurich, Radiocarbon, 66, 1054–1063, https://doi.org/10.1017/RDC.2023.16, 2024.

Castrillejo, M., Lherminier, P., Pérez, F. F., et al.: Author-provided supplemental seawater DIC Δ^{14}C for GO-SHIP sections A25 (2018) and A05 (2020), supplemental tables shared directly with the compilers; public release forthcoming. Processed in castrillejo_radiocarbon.ipynb., 2026.

Danabasoglu, G., Lamarque, J. F., Bacmeister, J., Bailey, D. A., DuVivier, A. K., Edwards, J., Emmons, L. K., Fasullo, J., Garcia, R., Gettelman, A., Hannay, C., Holland, M. M., Large, W. G., Lauritzen, P. H., Lawrence, D. M., Lenaerts, J. T. M., Lindsay, K., Lipscomb, W. H., Mills, M. J., Neale, R., Oleson, K. W., Otto-Bliesner, B., Phillips, A. S., Sacks, W., Tilmes, S., van Kampenhout, L., Vertenstein, M., Bertini, A., Dennis, J., Deser, C., Fischer, C., Fox-Kemper, B., Kay, J. E., Kinnison, D., Kushner, P. J., Larson, V. E., Long, M. C., Mickelson, S., Moore, J. K., Nienhouse, E., Polvani, L., Rasch, P. J., and Strand, W. G.: The Community Earth System Model Version 2 (CESM2), Journal of Advances in Modeling Earth Systems, 12, e2019MS001 916, https://doi.org/10.1029/2019MS001916, 2020.

DeLong, K. L., Kilbourne, K. H., Guilderson, T. P., Wagner, A. J., Slowey, N., Palmer, K., and Hajdas, I.: New and old coral radiocarbon records revisited for the subtropical and tropical Atlantic Ocean, Radiocarbon, 67, 487–512, 2025.

Druffel, E. M.: Radiocarbon in annual coral rings from the eastern Tropical Pacific Ocean, Geophysical Research Letters, 8, 59–62, https://doi.org/10.1029/GL008i001p00059, 1981.

Druffel, E. M. and Linick, T. W.: Radiocarbon in annual coral rings of Florida, Geophys. Res. Lett.; (United States), 5, 913–916, https://doi.org/10.1029/GL005i011p00913, 1978.

Druffel, E. R.: Geochemistry of corals: Proxies of past ocean chemistry, ocean circulation, and climate, Proceedings of the National Academy of Sciences, 94, 8354–8361, 1997.

https://doi.org/10.5194/essd-2026-691
Preprint. Discussion started: 27 August 2026

Druffel, E. R. M.: Decade time scale variability of ventilation in the North Atlantic: High-precision measurements of bomb radiocarbon in banded corals, Journal of Geophysical Research: Oceans, 94, 3271–3285, https://doi.org/10.1029/JC094iC03p03271, 1989.

Druffel, E. R. M. and Griffin, S.: Large variations of surface ocean radiocarbon: Evidence of circulation changes in the southwestern Pacific, Journal of Geophysical Research: Oceans, 98, 20 249–20 259, https://doi.org/10.1029/93JC02113, 1993.

Druffel, E. R. M., Williams, P. M., Bauer, J. E., and Ertel, J. R.: Cycling of dissolved and particulate organic matter in the open ocean, Journal of Geophysical Research: Oceans, 97, 15 639–15 659, https://doi.org/10.1029/92JC01511, 1992.

Druffel, E. R. M., Griffin, S., Glynn, D. S., Dunbar, R. B., Mucciarone, D. M., and Toggweiler, J. R.: Seasonal radiocarbon and oxygen isotopes in a Galapagos coral: Calibration with climate indices, Geophysical Research Letters, 41, 5099–5105, https://doi.org/10.1002/2014GL060504, 2014.

Druffel, E. R. M., Griffin, S., Vetter, D., Dunbar, R. B., and Mucciarone, D. M.: Identification of frequent La Niña events during the early 1800s in the east equatorial Pacific, Geophysical Research Letters, 42, 1512–1519, https://doi.org/10.1002/2014GL062997, 2015.

Druffel, E. R. M., Griffin, S., Glynn, C. S., Benner, R., and Walker, B. D.: Radiocarbon in dissolved organic and inorganic carbon of the Arctic Ocean, Geophysical Research Letters, 44, 2369–2376, https://doi.org/10.1002/2016GL072138, 2017.

Dutta, K., Bhushan, R., and Somayajulu, B. L. K.: ΔR Correction Values for the Northern Indian Ocean, Radiocarbon, 43, 483–488, https://doi.org/10.1017/S0033822200038376, 2001.

Fairhall, A. W. and Young, A. W.: Historical ^{14}C Measurements from the Atlantic, Pacific and Indian Oceans, Radiocarbon, 27, 473–507, http://hdl.handle.net/10150/652696, 1985.

Fallon, S. J. and Guilderson, T. P.: Extracting growth rates from the nonlaminated coralline sponge Astrosclera willeyana using bomb radiocarbon, Limnology and Oceanography: Methods, 3, 455–461, 2005.

Frischknecht, T., Ekici, A., and Joos, F.: Radiocarbon in the Land and Ocean Components of the Community Earth System Model, Global Biogeochemical Cycles, 36, e2021GB007 042, https://doi.org/10.1029/2021GB007042, 2022.

Goodkin, N. F., Druffel, E. R. M., Hughen, K. A., and Doney, S. C.: Two centuries of limited variability in subtropical North Atlantic thermocline ventilation, Nature Communications, 3, 803, https://doi.org/10.1038/ncomms1811, 2012.

Graven, H.: Atmospheric $\Delta^{14}CO_2$ forcing for input4MIPs (source ID: ImperialCollege-3-0), https://doi.org/10.25981/ESGF.input4MIPs.CMIP7/2583902, dataset landing page: https://input4mips-cvs.readthedocs.io/en/latest/source-id-landing-pages/ImperialCollege-3-0/, 2025.

Graven, H., Kozyr, A., and Key, R.: Historical observations of oceanic radiocarbon conducted prior to GEOSECS, https://doi.org/10.3334/CDIAC/OTG.HIST_C14_OBS, accessed 30 June 2026., 2012a.

Graven, H., Allison, C. E., Etheridge, D. M., Hammer, S., Keeling, R. F., Levin, I., Meijer, H. A. J., Rubino, M., Tans, P. P., Trudinger, C. M., Vaughn, B. H., and White, J. W. C.: Compiled records of carbon isotopes in atmospheric CO2 for historical simulations in CMIP6, Geosci. Model Dev., 10, 4405–4417, https://doi.org/10.5194/gmd-10-4405-2017, gMD, 2017.

Graven, H. D.: Impact of fossil fuel emissions on atmospheric radiocarbon and various applications of radiocarbon over this century, Proceedings of the National Academy of Sciences, 112, 9542–9545, https://doi.org/10.1073/pnas.1504467112, 2015.

Graven, H. D., Gruber, N., Key, R., Khatiwala, S., and Giraud, X.: Changing controls on oceanic radiocarbon: New insights on shallow-to-deep ocean exchange and anthropogenic CO_2 uptake, Journal of Geophysical Research: Oceans, 117, https://doi.org/10.1029/2012JC008074, 2012b.

Graven, H. D., Guilderson, T. P., and Keeling, R. F.: Observations of radiocarbon in CO_2 at La Jolla, California, USA 1992–2007: Analysis of the long-term trend, Journal of Geophysical Research: Atmospheres, 117, D02 302, https://doi.org/10.1029/2011JD016533, 2012c.

https://doi.org/10.5194/essd-2026-691
Preprint. Discussion started: 27 August 2026

Grottoli, A. G.: Monthly resolved stable oxygen isotope record in a Palauan sclerosponge Acanthocheatetes wellsi for the period of 1977–2001, in: Proc 10th Int Coral Reef Symp, vol. 2004, pp. 572–579, 2006.

Grottoli, A. G. and Eakin, C. M.: A review of modern coral δ18O and Δ14C proxy records, Earth-Science Reviews, 81, 67–91, 2007.

Guilderson, T. P. and Schrag, D. P.: Abrupt Shift in Subsurface Temperatures in the Tropical Pacific Associated with Changes in El Niño, Science, 281, 240–243, https://doi.org/10.1126/science.281.5374.240, 1998.

Hua, Q., Barbetti, M., and Rakowski, A. Z.: Atmospheric Radiocarbon for the Period 1950–2010, Radiocarbon, 55, 2059–2072, https://doi.org/10.2458/azu_js_rc.v55i2.16177, 2013.

Johnson, G. C., Robbins, P. E., and Hufford, G. E.: Systematic Adjustments of Hydrographic Sections for Internal Consistency, Journal of Atmospheric and Oceanic Technology, 18, 1234–1244, https://doi.org/10.1175/1520-0426(2001)018<1234:SAOHSF>2.0.CO;2, 2001.

Kaizer, J., Kumamoto, Y., Molnár, M., Palcsu, L., and Povinec, P. P.: Temporal changes in tritium and radiocarbon concentrations in the western North Pacific Ocean (1993–2012), Journal of Environmental Radioactivity, 218, 106 238, https://doi.org/10.1016/j.jenvrad.2020.106238, 2020.

Key, R. M., Kozyr, A., Sabine, C. L., Lee, K., Wanninkhof, R., Bullister, J. L., Feely, R. A., Millero, F. J., Mordy, C., and Peng, T. H.: A global ocean carbon climatology: Results from Global Data Analysis Project (GLODAP), Global Biogeochemical Cycles, 18, https://doi.org/10.1029/2004GB002247, 2004.

Kilbourne, K. H., Quinn, T. M., Guilderson, T. P., Webb, R. S., and Taylor, F. W.: Decadal- to interannual-scale source water variations in the Caribbean Sea recorded by Puerto Rican coral radiocarbon, Climate Dynamics, 29, 51–62, https://doi.org/10.1007/s00382-007-0224-2, 2007.

Kumamoto, Y., Murata, A., Saito, C., Honda, M., and Kusakabe, M.: Bomb radiocarbon invasion into the northwestern North Pacific, Deep Sea Research Part II: Topical Studies in Oceanography, 49, 5339–5351, https://doi.org/10.1016/S0967-0645(02)00194-7, 2002.

Lange, N., Lauvset, S. K., Carter, B. R., Humphreys, M. P., Woosley, R. J., Olsen, A., Bittig, H. C., Kozyr, A., Álvarez, M., Azetsu-Scott, K., Becker, S., Brown, P. J., Cotrim da Cunha, L., Hoppema, M., Ishii, M., Jeansson, E., Murata, A., Müller, J. D., Pérez, F. F., Schirnick, C., Steinfeldt, R., Ulfsbo, A., Velo, A., and Tanhua, T.: The Global Ocean Data Analysis Project version 3 (GLODAPv3) – an internally consistent biogeochemical data product for the World Ocean (NCEI Accession 0315582), https://doi.org/10.25921/m6tp-mj50, dataset; accessed 20 July 2026, 2026.

Lauvset, S. K., Lange, N., Tanhua, T., Bittig, H. C., Olsen, A., Kozyr, A., Álvarez, M., Azetsu-Scott, K., Brown, P. J., Carter, B. R., Cotrim da Cunha, L., Hoppema, M., Humphreys, M. P., Ishii, M., Jeansson, E., Murata, A., Müller, J. D., Pérez, F. F., Schirnick, C., Steinfeldt, R., Suzuki, T., Ulfsbo, A., Velo, A., Woosley, R. J., and Key, R. M.: The annual update GLODAPv2.2023: the global interior ocean biogeochemical data product, Earth Syst. Sci. Data, 16, 2047–2072, https://doi.org/10.5194/essd-16-2047-2024, 2024.

Lee, J.-M., Eltgroth, S. F., Boyle, E. A., and Adkins, J. F.: The transfer of bomb radiocarbon and anthropogenic lead to the deep North Atlantic Ocean observed from a deep sea coral, Earth and Planetary Science Letters, 458, 223–232, https://doi.org/10.1016/j.epsl.2016.10.049, 2017.

Lester, J. G., Graven, H. D., Khatiwala, S., and McNichol, A. P.: Changes in Oceanic Radiocarbon and CFCs Since the 1990s, Journal of Geophysical Research: Oceans, 129, e2023JC020 387, https://doi.org/10.1029/2023JC020387, 2024.

Levin, I. and Hesshaimer, V.: Radiocarbon – A Unique Tracer of Global Carbon Cycle Dynamics, Radiocarbon, 42, 69–80, https://doi.org/10.1017/S0033822200053066, 2000.

Levin, I., Naegler, T., Kromer, B., Diehl, M., Francey, R. J., Gomez-Pelaez, A. J., Steele, L. P., Wagenbach, D., Weller, R., and Worthy, D. E.: Observations and modelling of the global distribution and long-term trend of atmospheric $^{14}CO_2$, Tellus B, 62, 26–46, https://doi.org/10.1111/j.1600-0889.2009.00446.x, 2010.

Linick, T. W.: La Jolla Measurements of Radiocarbon in the Oceans, Radiocarbon, 20, 333–359, https://doi.org/10.1017/S0033822200009164, 1978.

Lower-Spies, E. E., Whitney, N. M., Wanamaker, A. D., Griffin, S. M., Introne, D. S., and Kreutz, K. J.: A 250-Year, Decadally Resolved, Radiocarbon Time History in the Gulf of Maine Reveals a Hydrographic Regime Shift at the End of the Little Ice Age, Journal of Geophysical Research: Oceans, 125, e2020JC016 579, https://doi.org/10.1029/2020JC016579, 2020.

Lu, Y., Wang, L., Wang, L., Cong, Y., Yang, G., and Zhao, L.: Deciphering carbon sources of mussel shell carbonate under experimental ocean acidification and warming, Marine environmental research, 142, 141–146, 2018.

Mamnun, N.: v1.0: Compilation code for a global ocean radiocarbon ($\Delta^{14}C$) dataset (1700–2024), https://doi.org/10.5281/zenodo.22100626, 2026.

Mamnun, N., Williams, B., Mukherjee, R., and Graven, H.: A Global Ocean Radiocarbon ($\Delta^{14}C$) Dataset (1700–2024) from Dissolved Inorganic Carbon and Marine Carbonate Archives, https://doi.org/10.5281/zenodo.22100029, 2026.

McConnaughey, T. A. and Gillikin, D. P.: Carbon isotopes in mollusk shell carbonates, Geo-Marine Letters, 28, 287–299, 2008.

Montero-Serrano, J.-C., Frank, N., Tisnerat-Laborde, N., Colin, C., Wu, C.-C., Lin, K., Shen, C.-C., Copard, K., Orejas, C., Gori, A., De Mol, L., Van Rooij, D., Reverdin, G., and Douville, E.: Decadal changes in the mid-depth water mass dynamic of the Northeastern Atlantic margin (Bay of Biscay), Earth and Planetary Science Letters, 364, 134–144, https://doi.org/10.1016/j.epsl.2013.01.012, 2013.

Nozaki, Y., Rye, D. M., Turekian, K. K., and Dodge, R. E.: A 200 year record of carbon-13 and carbon-14 variations in a Bermuda coral, Geophysical Research Letters, 5, 825–828, https://doi.org/10.1029/GL005i010p00825, 1978.

Nydal, R., Brenkert, A. L., and Boden, T. A.: Carbon-14 Measurements in Surface Water CO_2 from the Atlantic, Indian and Pacific Oceans, 1965–1994, https://doi.org/10.3334/CDIAC/otg.ndp057, accessed 30 June 2026., 1998.

Olsen, A., Key, R. M., van Heuven, S., Lauvset, S. K., Velo, A., Lin, X., Schirnick, C., Kozyr, A., Tanhua, T., Hoppema, M., Jutterström, S., Steinfeldt, R., Jeansson, E., Ishii, M., Pérez, F. F., and Suzuki, T.: The Global Ocean Data Analysis Project version 2 (GLODAPv2) – an internally consistent data product for the world ocean, Earth Syst. Sci. Data, 8, 297–323, https://doi.org/10.5194/essd-8-297-2016, 2016.

Östlund, H. G. and Stuiver, M.: GEOSECS Pacific Radiocarbon, Radiocarbon, 22, 25–53, https://doi.org/10.1017/S0033822200004707, 1980.

Pookkandy, B., Graven, H., and Martin, A. P.: Contemporary oceanic radiocarbon response to ocean circulation changes, Climate Dynamics, 61, 3223–3235, https://doi.org/10.1007/s00382-023-06737-3, 2023.

Rafter, P. A., Sanchez, S. C., Ferguson, J., Carriquiry, J. D., Druffel, E. R. M., Villaescusa, J. A., and Southon, J. R.: Eastern tropical North Pacific coral radiocarbon reveals North Pacific Gyre Oscillation (NPGO) variability, Quaternary Science Reviews, 160, 108–115, https://doi.org/10.1016/j.quascirev.2017.02.002, 2017.

Rafter, P. A., Gray, W. R., Hines, S. K. V., Burke, A., Costa, K. M., Gottschalk, J., Hain, M. P., Rae, J. W. B., Southon, J. R., Walczak, M. H., Yu, J., Adkins, J. F., and DeVries, T.: Global reorganization of deep-sea circulation and carbon storage after the last ice age, Science Advances, 8, eabq5434, https://doi.org/10.1126/sciadv.abq5434, 2022.

Rodgers, K. B., Lee, S.-S., Rosenbloom, N., Timmermann, A., Danabasoglu, G., Deser, C., Edwards, J., Kim, J.-E., Simpson, I. R., Stein, K., Stuecker, M. F., Yamaguchi, R., Bódai, T., Chung, E.-S., Huang, L., Kim, W. M., Lamarque, J.-F., Lombardozzi, D. L.,

https://doi.org/10.5194/essd-2026-691
Preprint. Discussion started: 27 August 2026

Wieder, W. R., and Yeager, S. G.: Ubiquity of human-induced changes in climate variability, Earth System Dynamics, 12, 1393–1411, https://doi.org/10.5194/esd-12-1393-2021, 2021.

Rosenheim, B. E. and Swart, P. K.: Caribbean sclerosponge radiocarbon measurements re-interpreted in terms of U/Th age models, Nuclear Instruments and Methods in Physics Research Section B: Beam Interactions with Materials and Atoms, 259, 474–478, 2007.

Schlosser, P., Kromer, B., Östlund, G., Ekwurzel, B., Bönisch, G., Loosli, H. H., and Purtschert, R.: On the 14C and 39Ar Distribution in the Central Arctic Ocean: Implications for Deep Water Formation, Radiocarbon, 36, 327–343, https://doi.org/10.1017/S003382220001451X, 1994.

Schlosser, P., Bauch, D., Fairbanks, R. G., and Bönisch, G.: Arctic Ocean Radiocarbon Record Between 1987 and 1994, Nuclear Instruments and Methods in Physics Research Section B: Beam Interactions with Materials and Atoms, 123, 431–437, https://doi.org/10.1016/S0168-583X(96)00677-5, 1997.

Scourse, J., Richardson, C., Forsythe, G., Harris, I., Heinemeier, J., Fraser, N., Briffa, K., and Jones, P.: First cross-matched floating chronology from the marine fossil record: data from growth lines of the long-lived bivalve mollusc Arctica islandica, The Holocene, 16, 967–974, 2006.

Scourse, J. D., Wanamaker, A. D., Weidman, C., Heinemeier, J., Reimer, P. J., Butler, P. G., Witbaard, R., and Richardson, C. A.: The Marine Radiocarbon Bomb Pulse Across the Temperate North Atlantic: A Compilation of $\Delta^{14}C$ Time Histories from Arctica Islandica Growth Increments, Radiocarbon, 54, 165–186, https://doi.org/10.2458/azu_js_rc.v54i2.16026, 2012.

Shen, C. D., Yi, W. X., Yu, K. F., Sun, Y. M., Yang, Y., and Zhou, B.: Interannual ^{14}C Variations During 1977–1998 Recorded in Coral from Daya Bay, South China Sea, Radiocarbon, 46, 595–601, https://doi.org/10.1017/S0033822200035633, 2004.

Sherwood, O. A., Scott, D. B., Risk, M. J., and Guilderson, T. P.: Radiocarbon evidence for annual growth rings in the deep-sea octocoral Primnoa resedaeformis, Marine Ecology Progress Series, 301, 129–134, https://doi.org/10.3354/meps301129, 2005.

Sherwood, O. A., Edinger, E. N., Guilderson, T. P., Ghaleb, B., Risk, M. J., and Scott, D. B.: Late Holocene radiocarbon variability in Northwest Atlantic slope waters, Earth and Planetary Science Letters, 275, 146–153, https://doi.org/10.1016/j.epsl.2008.08.019, 2008.

Skinner, L. C. and Bard, E.: Radiocarbon as a Dating Tool and Tracer in Paleoceanography, Reviews of Geophysics, 60, https://doi.org/10.1029/2020rg000720, 2022.

Stuiver, M. and Polach, H. A.: Discussion: Reporting of ^{14}C Data, Radiocarbon, 19, 355–363, https://doi.org/10.1017/S0033822200003672, 1977.

Swart, P., Thorrold, S., Rosenheim, B., Eisenhauer, A., Harrison, C., Grammer, M., and Latkoczy, C.: Intra-annual variation in the stable oxygen and carbon and trace element composition of sclerosponges, Paleoceanography, 17, 17–1, 2002.

Talley, L. D., Feely, R. A., Sloyan, B. M., Wanninkhof, R., Baringer, M. O., Bullister, J. L., Carlson, C. A., Doney, S. C., Fine, R. A., Firing, E., Gruber, N., Hansell, D. A., Ishii, M., Johnson, G. C., Katsumata, K., Key, R. M., Kramp, M., Langdon, C., Macdonald, A. M., Mathis, J. T., McDonagh, E. L., Mecking, S., Millero, F. J., Mordy, C. W., Nakano, T., Sabine, C. L., Smethie, W. M., Swift, J. H., Tanhua, T., Thurnherr, A. M., Warner, M. J., and Zhang, J.-Z.: Changes in Ocean Heat, Carbon Content, and Ventilation: A Review of the First Decade of GO-SHIP Global Repeat Hydrography, Annual Review of Marine Science, 8, 185–215, https://doi.org/10.1146/annurev-marine-052915-100829, 2016.

Vogel, J. C. and Marais, M.: Pretoria Radiocarbon Dates I, Radiocarbon, 13, 378–394, https://doi.org/10.1017/S003382220000850X, 1971.

Wang, N., Shen, C., Sun, W., Yi, W., Ding, P., Ding, X., Fu, D., and Liu, K.: Seasonal 14C and Sr/Ca Records of a Modern Coral around Daya Bay Nuclear Power Plants, Radiocarbon, 59, 1035–1046, https://doi.org/10.1017/RDC.2017.43, 2017.

Weidman, C. R.: North Atlantic Mollusc Isotope Data, 1995.

https://doi.org/10.5194/essd-2026-691
Preprint. Discussion started: 27 August 2026

Williams, B. and Grottoli, A. G.: Recent shoaling of the nutricline and thermocline in the western tropical Pacific, Geophysical Research Letters, 37, L22 601, https://doi.org/10.1029/2010GL044867, 2010.